Document made available under the Patent Cooperation Treaty (PCT)

International application number: PCT/CA04/002119

International filing date: 13 December 2004 (13.12.2004)

Document type: Certified copy of priority document

Document details: Country/Office: US
Number: 60/528,723
Filing date: 12 December 2003 (12.12.2003)

Date of receipt at the International Bureau: 30 March 2005 (30.03.2005)

Remark: Priority document submitted or transmitted to the International Bureau in compliance with Rule 17.1(a) or (b)

PCT/CA 04002119

PA 1273275

THE UNITED STATES OF AMERICA

TO ALL TO WHOM THESE PRESENTS SHALL COME:

UNITED STATES DEPARTMENT OF COMMERCE

United States Patent and Trademark Office

January 19, 2005

THIS IS TO CERTIFY THAT ANNEXED HERETO IS A TRUE COPY FROM THE RECORDS OF THE UNITED STATES PATENT AND TRADEMARK OFFICE OF THOSE PAPERS OF THE BELOW IDENTIFIED PATENT APPLICATION THAT MET THE REQUIREMENTS TO BE GRANTED A FILING DATE UNDER 35 USC 111.

APPLICATION NUMBER: *60/528,723*
FILING DATE: *December 12, 2003*

By Authority of the
COMMISSIONER OF PATENTS AND TRADEMARKS

E. Bornett

E. BORNETT
Certifying Officer

UNITED STATES PATENT AND TRADEMARK OFFICE
DEPARTMENT OF COMMERCE

16698 U.S. PTO

Please type a plus sign (+) inside this box → ☐

PTO/SB/16 (5-03)
Approved for use through 4/30/2003. OMB 0651-0032
U.S. Patent and Trademark Office; U.S. DEPARTMENT OF COMMERCE
Under the Paperwork Reduction Act of 1995, no persons are required to respond to a collection of information unless it displays a valid OMB control number.

PROVISIONAL APPLICATION FOR PATENT COVER SHEET

This is a request for filing a PROVISIONAL APPLICATION FOR PATENT under 37 CFR 1.53(c).

17510 U.S. PTO 60/528723 121203

INVENTOR(S)

Given Name (first and middle [if any])	Family Name or Surname	Residence (City and either State or Foreign Country)
Gro	Thorne-Tjomsland	Winnipeg Manitoba Canada

☐ *Additional inventors are being named on the ____ separately numbered sheets attached hereto*

TITLE OF THE INVENTION (280 characters max)

Regulation of Very Low Density Lipoprotein (VLDL) Assembly in Post-Endoplasmic Reticulum of Rat Hepatoma McA-RH7777Cells

Direct all correspondence to: **CORRESPONDENCE ADDRESS**

☒ Customer Number **23529** →
Type Customer Number here

Place Customer Number Bar Code Label here

OR

☒ Firm *or* Individual Name	ADE & COMPANY				
Address	1700-360 Main Street				
Address					
City	Winnipeg	State	Manitoba	ZIP	R3C 3Z3
Country	Canada	Telephone	204-947-1429	Fax	204-942-5723

ENCLOSED APPLICATION PARTS *(check all that apply)*

☒ Specification *Number of Pages* **38**
☒ Drawing(s) *Number of Sheets* **12**
☐ Application Data Sheet. See 37 CFR 1.76
☐ CD(s), Number
☐ Other (specify)

METHOD OF PAYMENT OF FILING FEES FOR THIS PROVISIONAL APPLICATION FOR PATENT *(check one)*

☒ Applicant claims small entity status. See 37 CFR 1.27.
☒ A check or money order is enclosed to cover the filing fees
☐ The Director is hereby authorized to charge filing fees or credit any overpayment to Deposit Account Number
☐ Payment by credit card. Form PTO-2038 is attached.

FILING FEE AMOUNT ($) **$80.00**

The invention was made by an agency of the United States Government or under a contract with an agency of the United States Government.
☒ No.
☐ Yes, the name of the U.S. Government agency and the Government contract number are: ____________

Respectfully submitted,

SIGNATURE

Date **11/12/03**

TYPED or PRINTED NAME **Michael R. Williams**

REGISTRATION NO. *(if appropriate)* **45,333**

TELEPHONE **204-957-8364**

Docket Number: **82402-7672**

USE ONLY FOR FILING A PROVISIONAL APPLICATION FOR PATENT

Regulation of Very Low Density Lipoprotein (VLDL) Assembly in Post-Endoplasmic Reticulum of Rat Hepatoma McA-RH7777 Cells

FIELD OF THE INVENTION

The present invention relates generally to the field of medical treatments. More specifically, the present invention relates to methods and compounds for modulating or reducing VLDL secretion.

BACKGROUND OF THE INVENTION

The liver secretes triglyceride (TG) in the form of very low density lipoprotein (VLDL) that are heterogeneous in size and metabolic fate (Packard and Shepherd, 1997, *Arterioscler.Thromb.Vasc.Biol.* **17,** 3542-3556). Each VLDL particle contains one copy of apolipoprotein (apo) B100 and various amount of TG (Fisher and Ginsberg, 2002, *J.Biol.Chem.* **277,** 17377-17380). In rat hepatoma McA-RH7777 cells, assembly of VLDL is accomplished post-translationally in a post-endoplasmic reticulum (ER) compartment (Tran et al., 2002, *J.Biol.Chem.* **277,** 31187-31200). After its synthesis, apoB100 exits the ER and traverses the *cis*/medial Golgi in a membrane-associated form associated with little lipids (Tran et al., 2002); complete assembly of bulk TG with apoB100 to form VLDL does not occur until apoB100 reaches the distal Golgi (Tran et al., 2002). Formation of the lipid-poor primordial lipoprotein particles in the ER is referred as first-step assembly, whereas incorporation of bulk TG into VLDL within post-ER compartments is known as second-step assembly (Rustaeus et al., 1999, *J.Nutr.* **129,** 463S-466S; Stillemark et al., 2000, *J.Biol.Chem.* **275,** 10506-10513). Factors affecting first-step assembly often govern folding of the nascent apoB100 polypeptide chain, either through post-translational modification (*e.g.* disulfide bond formation (Tran et al., 1998, *J.Biol.Chem* **273,** 7244-7251) or N-linked glycosylation (Vukmirica et al., 2002, *J.Lipid Res.* **43,** 1496-1507)) or through the interaction of apoB100 with microsomal triglyceride transfer protein (MTP) (Dashti et al., 2002, *Biochemistry* **41,** 6978-6987). Recently, a point mutation R463W associated with familial hypobetalipoproteinemia was identified within the MTP-binding region of apoB that causes impaired first-step assembly (Burnett et al., 2003, *J.Biol.Chem.* **278,** 13442-

13452). Features associated with attenuated first-step assembly include enhanced intracellular degradation of newly synthesized apoB100 and decreased secretion of apoB100 proteins. Degradation of misfolded nascent apoB100 in the ER is usually mediated by the ubiquitin-proteosomal system (Fisher and Ginsberg, 2002; Yao et al., 1997, *J.Lipid Res* **38,** 1937-1953).

On the other hand, factors affecting second-step assembly are generally of a lipid nature. Increasing experimental evidence suggests that phospholipid composition of membranes along the secretory pathway is an important determinant of second-step assembly. Previous studies using agents that perturb membrane phospholipid composition by directly (Asp et al., 2000, *J.Biol.Chem.* **275,** 26285-26292; Nishimaki-Mogami et al., 2002, *J.Lipid Res.* **43,** 1035-1045; Tran et al., 2000, *J.Biol.Chem* **275,** 25023-25030) or indirectly (McLeod et al., 1996, *J.Biol.Chem.* **271,** 18445-18455; Wang et al., 1999, *J.Biol.Chem.* **274,** 27793-27800; Yao and Vance, 1988, *J.Biol.Chem.* **263,** 2998-3004) altering the activity of phospholipid-modifying enzymes have identified several such factors. Among them are phosphatidylcholine (PC) and phosphatidylethanolamine (PE) species enriched with oleoyl (18:1(n-9)) chains that create a microsomal membrane milieu permissive to VLDL assembly (Tran et al., 2000). Formation of 18:1(n-9)-rich phospholipid species can be achieved through phospholipid remodeling (*i.e.*, deacylation and reacylation) mediated in part by calcium-independent phospholipase A_2 (iPLA_2) in liver cells (Tran et al., 2000). Turnover of these phospholipids also donates 18:1(n-9) acyl chain for TG synthesis (Tran et al., 2000) and for formation of signaling molecules such as 18:1(n-9)-phosphatidic acid and 18:1(n-9)-diglyceride that play a key role in membrane movement and fusion(Antonny et al., 1997, *J.Biol.Chem.* **272,** 30848-30851; Chernomordik et al., 1995, *J.Membr.Biol.* **146,** 1-14). Limiting incorporation of 18:1(n-9) into membrane phospholipid by oleate deprivation (McLeod et al., 1996), reducing phospholipid remodeling by iPLA_2 inhibition (Tran et al., 2000), and decreasing formation of phosphatidic acid by inhibition of ADP-ribosylation factor-dependent phospholipase (D Asp et al., 2000) in McA-RH7777 cells invariably result in reduced VLDL assembly at the second step. The hallmark of impaired second-step assembly is the secretion of dense, TG-poor apoB100-containing lipoproteins (LpBs). Secretion-incompetent LpBs are destined for degradation by a yet unknown

mechanism. A non-proteosomal and post-ER degradation mechanism has been postulated to eliminate abnormal LpBs formed after apoB exits the ER (i.e., in second-step assembly) under various conditions (Fisher et al., 2001, J.Biol.Chem. 276, 27855-27863; Phung et al., 1997, J.Biol.Chem. 272, 30693-30702; Wang et al., 1995, J.Biol.Chem. 270, 24924-24931). Molecular details of this mechanism for apoB degradation are currently unclear. It has been suggested that non-proteasomal degradation occurs in a low density microsome compartment distinct from ER or Golgi (Phung et al., 1997, J.Biol.Chem. 272, 30693-30702) and is sensitive to inhibition of phosphatidylinositide 3-kinase (Fisher et al., 2001, *J.Biol.Chem.* **276,** 27855-27863; Phung et al., 1997, *J.Biol.Chem.* **272,** 30693-30702).

In the present study, the impact of membrane phospholipid remodeling on second-step VLDL assembly was investigated by comparing oleate with eicosapentaenoic acid (EPA, 20:5(n-3)). The inhibitory effect on TG secretion *in vitro* (Lang and Davis, 1990, *J.Lipid Res.* **31,** 2079-2086; Wong and Nestel, 1987, *Atherosclerosis* **64,** 139-146) and the plasma TG-lowering effect of EPA *in vivo* (Harris, 1999, *Lipids* **34 Suppl,** S257-S258) have been documented. However, the mechanism of the hypotriglyceridemic effect of EPA has not been clearly elucidated and remains controversial. We hypothesize that incorporation of 20:5(n-3) into phospholipid and subsequently into TG through remodeling creates a lipid environment unfavorable for second-step VLDL assembly. To test this hypothesis, McA-RH7777 cells expressing human apoB100 were cultured under conditions where synthesis and ER exit of apoB100 were unaffected by the EPA treatment. The current data showed that alteration in phospholipid molecular species by exogenous fatty acids appears to affect the recruitment of TG, which is modulated by its synthesis and intracellular distribution, during second-step VLDL assembly, and to coincide with formation of post-ER degradative compartment.

SUMMARY OF THE INVENTION

According to a first aspect of the invention, there is provided a method of inducing reducing serum levels of triglycerides and/or very low density lipoprotein comprising administering to an individual in need of such treatment an effective amount

of an autophagolysosome inducing compound.

According to a second aspect of the invention, there is provided a pharmaceutical composition capable of inhibiting autophagocytosis selected from the group consisting of wortmannin, 3 methyladenine, LY294002, Class I P13'kinase and rapamycin.

According to a third aspect of the invention, there is provided a pharmaceutical composition capable of inducing autophagocytosis selected from the group consisting of Map1LC3, GABARAP, GATE16 and Class III P13'kinase.

BRIEF DESCRIPTION OF THE DRAWINGS

FIG. 1. **EPA treatment induced formation and secretion of dense apoB100-containing lipoproteins.** *A*, Cells pretreated with oleate or EPA for 16 h were pulse-labeled with [^{35}S]methionine/cysteine for 30 min and chased for 1 h. The conditioned medium (*top panel*) or lumenal content of total microsomes (*bottom panel*) was subjected to rate flotation centrifugation as described in the "Experimental Procedures." The ^{35}S-apoB100 in each fraction was immunoprecipitated and resolved by SDS-PAGE/fluorography. *B*, Cells pretreated with oleate and EPA were pulse labeled with [^{35}S]methionine/cysteine for 1 h and chased for up to 3 h. Oleate and EPA were present in both pulse and chase. The [^{35}S]apoB100 (*top panels*) and [^{35}S]apoA-I (*bottom panels*) from total cell lysates (*left top and bottom panels*) or conditioned media (*right top and bottom panels*) were immunuprecipitated and resolved by SDS-PAGE/fluorography. The data were expressed as percent of the initial incorporated counts after 30-min pulse.

FIG. 2. **Intracellular trafficking of membrane-associated apoB100 and formation of apoB100-containing lipoproteins in the lumen of ER/Golgi.** Cells pretreated with oleate or EPA were pulse labeled with [^{35}S]methionine/cysteine for 20 min and chased from 0-45 min. The subcellular compartments were fractionated by Nycodenz gradient centrifugation, and membranes (*A*, at various chase times) and lumenal content (*B*, at 45 min chase) of ER, *cis*/medial Golgi, and distal Golgi were isolated by sodium carbonate treatment followed by ultracentrifugation. The ^{35}S-apoB100 was

immunoprecipitated and resolved by SDS-PAGE/fluorography as described in the "Experimental Procedures".

FIG. 3. **Immunofluorescent localization of apoB and Map1LC3.** Cells pretreated with none (*control*), oleate or EPA were permeabilized and blotted with anti-human apoB antibody (apoB) and anti-rat Map1LC3 antibody (Map1LC3), respectively. The secondary antibody for apoB was conjugated with Alexa Fluor™488 (green), and that for Map1LC3 was conjugated with Alexa Fluor™594 (red). The *circles* in the merge images show redistribution of Map1LC3 into the apoB-rich region in oleate- or EPA-treated cells. *Arrowheads* show co-localization of Map1LC3 and apoB (magnified in *insets*). Scale bar, 10 μm.

FIG. 4. **Fluorescent labeling of monodansylcadaverine (MDC) and low magnification TEM.** *A*, monodansylcadaverine (MDC)-labeling of control, oleate- and EPA-treated cells. Scale bar, 10 μm. *B*, TEM of control, oleate- and EPA-treated cells. *Large arrows* denote dense vacuoles near the Golgi apparatus (*GA*; stippled). *Small arrows* denote small dense vacuoles within the Golgi region of oleate- or EPA-treated cells. Nucleus (*N*); lipid droplets (*L*).

FIG. 5. **Five types of lipid/lipoprotein particles identified in the Golgi and associated vacuoles** The Golgi in *A,B,C* each have 4 saccules [1-4; note saccule 1 contains characteristic perforations (arrowheads) and is closely associated with overlaying ER]. *A* and *B* also shows a *trans*-Golgi network (TGN) and *C*, a large *trans*-Golgi associated vacuole (note partial encasement by cisternal membrane, *dotted line*). The particles detected in the Golgi and associated vacuoles were classified into five types (I-V, *A-C*), seen at higher magnification in *D*. Type I, II and III particles have a peripheral "halo" (*brackets*, D, top panel) and respectively a large (*large white asterisk, D*), "shrinking" (*large white asterisks, D*) and empty (*large black asterisks,* D) core. A phospholipid monolayer (*arrows, D*) is detected between the halo and core of Type II and III particles. Type II particles have porosities (*small asterisks*, D) in the core, just deep to the phospholipid monolayer. Thin strands of material [*arrowheads*, *D*; *E* (middle

image)] span these porosities from the electron-dense core to the phospholipid membrane. Type IV (*white arrowheads*, D, middle panel) and V (*D*, lower panel) are respectively small (<25 nm diameter) and large (>25 nm diameter) spheroid, electron-dense, homogeneous particles. Note that in the Golgi, Type I-V particles occur either singly (*A-C*) or in pairs (*boxes, B*), whereas in vacuoles, particles are frequently seen in "rosettes" of a single Type I, II or III particle surrounded by several Type IV/V particles (*boxes*, C). *E*, Rosettes consisting of respectively a single Type I, II or III particle and multiple Type IV/V particles.

FIG. 6. **Transmission electron microscopy shows formation of lipid/lipoprotein-containing vacuoles in the *trans*-Golgi region of EPA-treated cells.** *A*, Two Golgi stacks (*GA1, GA2*) display respectively four and five saccules [1-5, saccule 1 contains large perforation (arrowheads)] and are associated with a small *trans*-Golgi network (*TGN*) and a secretory vesicle (*SV*). Electron-dense particles of which the morphometric data were shown in Fig. 5 likely correspond to a combination of lipid/lipoprotein particles seen in the Golgi/TGN/SV. Similar particles (*A-C, double, short and long arrows*) are seen in a number of vacuoles (*A-C, small asterisks*) located near the Golgi. Most of these vacuoles are encased by cisternal membranes (*dotted lines*) which display some ribosomes (*arrowheads*), and hence appear to be ER-derived. Large vacuoles (*large asterisks*) located further away from the Golgi have a dense, indeterminate content. Scale bar, 1 µm. *B*, Three vacuoles (*black asterisks*), located near the *trans*-side of a small Golgi (*GA*), are partially encased by cisternal membranes (*dotted lines*). Ring-shaped, small and large sheroid particles (*double-*, *short- and long-arrows*, respectively) are identified in the vavuoles. The limiting membrane of the vacuole shown at bottom has two buds (*white arrows*) and an invagination, which accommodates several small vesicles and tubules (*white asterisks*). *Arrowheads* denote microtubules. Scale bar, 0.4 µm. *C*, In this group of vacuoles, some contain (*small asterisks*) and some don't contain (*large asterisks*) electron-dense particles (*arrows*). Note close association and apparent fusion (*white arrowheads*) between a vacuole containing and a vacuole not containing recognizable lipid/lipoprotein particles. *D*, 3D model shows two Golgi stacks (*cis*-most Golgi saccule, *yellow*; saccules 2-5, *grey*; TGN/SV, *orange*) and a group of vacuoles

(*medium blue*) between them, which all contained recognizable lipid/lipoproteins at the serial section level. Several of these vacuoles show invaginations in their limiting membranes, which accommodate small vesicles/tubules (*royal blue*). Apparent fusion between adjacent vacuoles (as in panel *C*) is indicated with black arrowheads. Dilations (*light blue*) containing electron-dense particles are continuous with *trans*-Golgi saccules; this continuity is evident (*arrows*) for the two dilations closest to the viewer. Perforation in *cis*-saccule (*white arrowhead*). *E*, Lower Golgi stack from Fig. 6*D* rotated 180° along the x-axis and modeled to include cisternal membranes (*red*). Particle-filled vacuoles (*medium blue*) which did not obscure the *trans*-Golgi were included in the model. Two of these (*1, *2) are seen in equatorial view and show association with cisternal membranes along their periphery. An additional two (*3, *4) are seen in "pole view", which gives a clearer view of the 3D encasement by cisternal membranes. Note cisternal membranes (*red*) also encase (*white stippled lines*) lipid/lipoprotein containing dilations (*light blue*) which are in direct continuity with *trans*-Golgi saccules in the regions shown (*arrows*), within the serial sections.

FIG. 7. **Analysis of PC and PE molecular species in the membrane of various intracellular compartments.** Membrane PC (*A*) and PE (*B*) molecular species from the experiments described in the legend of Table II were determined by daughter ion analysis. The data were plotted as peak areas that have been normalized with the values of the internal standards, dimyristoyl (*14:0-14:0)-PC and dipalmitoyl (*16:0-16:0)-PE for PC and PE species, respectively.

FIG. 8. **Redistribution of incorporated [^{14}C]oleate and [^{3}H]EPA among cellular lipids.** Cells were labeled with [^{14}C]oleate or [^{3}H]EPA for 2 h, and incubated in the presence or absence of 0.4 mM exogenous oleate or EPA, respectively, for indicated times (chase time). After each chase time, total lipids of the cells were extracted and lipid classes were resolved and determined by TLC. The data were averages of two independent experiments and expressed as percent of total radioactivities incorporated after 2-h labeling, which were 2.4 x 10^6 and 6.1 x 10^5 cpm for [^{14}C]oleate and [^{3}H]EPA, respectively. The error bars were deviation from the means.

FIG. 9. **Secretion of lipids containing [^{14}C]oleate and [^{3}H]EPA.** The experimental conditions were identical to those stated in figure 5, except total lipids in the medium of each chase time were extracted and lipid classes were resolved and determined by TLC. The data were averages of two independent experiments and expressed as percent of total radioactivity incorporated after 2-h labeling. The error bars were deviation from the means. FA, free fatty acids.

FIG. 10. **Compartmentalization of incorporated [^{14}C]oleate and [^{3}H]EPA among cellular lipids.** Cells were labeled with or without [^{14}C]oleate (*A*) and with or without [^{3}H]EPA (*B*) for 2 h, and incubated in the absence (*open bars*) or presence (*closed bars*) of 0.4 mM exogenous oleate or EPA, respectively, for 4 h (chase time). The cells were homogenized and the intracellular compartments (*i.e.* cytosol, microsomal membranes, microsomal lumen and nuclei/mitochondria) were isolated. Total lipids were extracted and lipid classes were resolved and determined by TLC. The data were averages of duplicates and expressed as percent of total radioactivity incorporated at the end of 2-h labeling. The deviations were equal or less than 5 % of the mean values. FA, free fatty acids.

FIG. 11. **Relationship between phospholipid remodeling/turnover and distribution of metabolically distinct TG pools.** Phospholipid remodeling/turnover provides acyl chain for TG synthesis that is occurred on both lumenal and cytosolic sides of the membrane bilayer. The C18:1(n-9) acyl chain derived from PC is assimilated into TG-18:1 whereas C20:5(n-3) acyl chain derived from PE is incorporated into TG-20:5. As compared with TG-18:1, TG-20:5 is preferentially formed on the cytosolic side and poorly utilized to package into VLDL in the lumenal side of the microsomal membranes. Secretion-incompetent lipoprotein and lipid particles are destined for degradation by autophagy.

DESCRIPTION OF THE PREFERRED EMBODIMENTS

Unless defined otherwise, all technical and scientific terms used herein have the

same meaning as commonly understood by one of ordinary skill in the art to which the invention belongs. Although any methods and materials similar or equivalent to those described herein can be used in the practice or testing of the present invention, the preferred methods and materials are now described. All publications mentioned hereunder are incorporated herein by reference.

As used herein, "effective amount" refers to the administration of an amount of a given compound that achieves the desired effect.

As used herein, the term "treating" in its various grammatical forms refers to preventing, curing, reversing, attenuating, alleviating, minimizing, suppressing or halting the deleterious effects of a disease state, disease progression, disease causitive agent or other abnormal condition.

Described herein is a mechanism whereby TG and/or VLDL secretion and/or concentration are modulated involving the formation of a post-ER degradative complex. Compounds which promote or inhibit autophagolysosome formation can be identified as discussed below. As will be apparent to one of skill in the art, these modulating compounds may be used as pharmaceuticals for the prevention and/or treatment of a number of cardiovascular diseases, including but by no means limited to hypercholesterolemia, hyperlipidemia, hyperlipoproteinemia, atherosclerosis, cardiovascular disorders, coronary heart disease, coronary artery disease; and strokes.

The molecular mechanism for inducing/initiating autophagocytosis is well characterized in yeast (Mizushima et al., 2003, Int. J. Biochem. and Cell Biology 35, 553-561), but less so in mammalian cells although some mammalian analogues have been identified for the yeast proteins, including Map1LC3 (microtubule associated protein 1 light chain 3/LC3), GABARAP (γ–aminobutyric acid(GABA)$_A$—receptor-associated protein and GATE-16 (Golgi-associated ATPase enhancer of 16kDa). X-ray and NMR structures, including preliminary ones, have recently been published for all three mammalian analogues. Mammalian analogues of the yeast proteins or sequences thereof, including Map1LC3 are possible agonists of autophagocytosis, and antibodies or inhibitors to these proteins are possible antagonists. Map1LC3 exists in two isoforms in the rat (I and II) with II being the active form binding to the membrane. Map1LC3

exists in three isoforms in humans, A, B and C; A and C exist both in a non-membrane bound and a membrane-bound (active) form, whereas B is not thought to only exist in a non-membrane-bound form. It is thought that both Map1LC3 and its' yeast analogue become covalently attached to phosphatidylethanolamine moieties within the membrane of autophagic membranes. Thus compounds which alter the amount/concentration of phoshatidylethanolamine in the membrane have the potential to affect autophagosome formation. Wortmannin, 3-methyladenine and LY294002 are known inhibitors of autophagocytosis, which inhibit phosphatidylinositol 3'kinases (PI3'kinases). Class I PI3'kinases are autophagocytosis antagonists and Class III PI3'kinases are known agonists of autophagocytosis. Rapamycin is a known inhibitor of autophagocytosis; this is a macrocyclic lacton which inhibits function of mTor (mammalian rapamycin target) a Ser/Thr kinase with homology to PI3'kinases.

Thus, compounds capable of inducing autophagocytosis and thereby reducing serum levels of TG and/or VLDL include but are by no means limited to Map1LC3, GABARAP, GATE16 and Class III P13'kinase. As will be appreciated by one of skill in the art, effective amounts of these compounds or mixtures thereof, alone or in combination with other suitable components, may be used in the production of pharmaceuticals for treating or preventing cardiovascular diseases, as discussed herein.

In yet other embodiments, these pharmaceutical compositions are administered to individuals in need thereof, for example, individuals suffering from or at risk of developing a cardiovascular disease. As discussed herein, an effective amount of at least one of these pharmaceutical compounds will reduce serum levels of TG and/or VLDL.

Compounds capable of inhibiting autophagocytosis include but are by no means limited to wortmannin, 3 methyladenine, LY294002, Class I P13'kinase and rapamycin.

In some embodiments, the autophagolysosome modulating compound may be combined with a pharmaceutically or pharmacologically acceptable carrier, excipient or diluent, either biodegradable or non-biodegradable. Exemplary examples of carriers include, but are by no means limited to, for example, poly(ethylene-vinyl acetate), copolymers of lactic acid and glycolic acid, poly(lactic acid), gelatin, collagen matrices,

polysaccharides, poly(D,L lactide), poly(malic acid), poly(caprolactone), celluloses, albumin, starch, casein, dextran, polyesters, ethanol, mathacrylate, polyurethane, polyethylene, vinyl polymers, glycols, mixtures thereof and the like. Standard excipients include gelatin, casein, lecithin, gum acacia, cholesterol, tragacanth, stearic acid, benzalkonium chloride, calcium stearate, glyceryl monostearate, cetostearyl alcohol, cetomacrogol emulsifying wax, sorbitan esters, polyoxyethylene alkyl ethers, polyoxyethylene castor oil derivatives, polyoxyethylene sorbitan fatty acid esters, polyethylene glycols, polyoxyethylene stearates, colloidol silicon dioxide, phosphates, sodium dodecylsulfate, carboxymethylcellulose calcium, carboxymethylcellulose sodium, methylcellulose, hydroxyethylcellulose, hydroxypropylcellulose, hydroxypropylmethycellulose phthalate, noncrystalline cellulose, magnesium aluminum silicate, triethanolamine, polyvinyl alcohol, polyvinylpyrrolidone, sugars and starches. See, for example, Remington: The Science and Practice of Pharmacy, 1995, Gennaro ed.

According to one aspect of the invention, there is provided a method of promoting formation of a post-ER degradative compartment comprising administering an effective amount of an autophagolysosome promoting compound, for example, but are by no means limited to Map1LC3, GABARAP, GATE16 and Class III P13'kinase.

As will be appreciated by one of skill in the art, this method could be carried out *in vivo* as a medical treatment or *in vitro* or *in situ* as a method for screening for compounds capable of promoting (or inhibiting) autophagolysosomes. In this manner, novel compounds that act either as agonists or antagonists of autophagolysosomes can be identified. The invention is further directed to such compounds isolated by these methods.

The invention is also directed to screening methods for identifying autophagolysosome modulating compounds. For example, one could test autophagocytosis-inducing compounds in a cell culture system, for example using cultured rat hepatocyte or rat hepatoma cells expressing human apoB100. One could assay for VLDL and its' precursors in ER and Golgi fractions as well as in the culture medium. Immunofluorescent microscopy, including confocal microscopy could be used to assay for the degree of co-localization of apoB100 and Map1LC3.

As will be appreciated by one of skill in the art, as used herein, "compounds" refers to small molecules, chemical compounds, biomolecules, synthetic peptides and the like. In these embodiments, compounds producing an abnormal result compared to untreated control cells, for example, reduced VLDL levels or abnormal co-localization of apoB100 and Map1LC3, indicates that the compound is capable of modulating autophagocytosis. The invention is also directed to compounds isolated by these or similar methods for identifying compounds capable of modulating autophagocytosis.

The invention is also directed to methods of treating diseases or disorders characterized by abnormal levels of TG and/or VLDL secretion or plasma concentration comprising altering the membrane phospholipids composition of a patient in need of such a treatment, as discussed herein.

The autophagic degradative pathway has been known for ~ 40 years (Ashford and Porter, 1962, J. Cell Biol. 12, 1982). It is essential for survival during starvation and cell differentiation because it degrades and recycles cytoplasmic components. It is thought to primarily degrade longer lived proteins in the cells, unlike the uqibuitin-proteasome pathway which degrades shorter lived proteins.

This work contributes the notion that the autophagic pathway has been adapted to sequester some shorter-lived proteins (immediately following synthesis or while still undergoing post-synthesis modifications) and macromolecular complexes, in this case lipid and lipoprotein particles.

It is known that cells can degrade the apolipoprotein component of lipoproteins during synthesis by the ubuiquitin-proteasome pathway. A second degradative pathway has been proposed to occur in a low density microsome compartment distinct from the endoplasmic reticulum (where apolipoproteins are synthesized/translated) and non-Golgi (where apolipoproteins are post-translationally modified), but had not been further identified or characterized.

Autophagocytosis can be upregulated/induced for example by nutrient starvation (amino acid withdrawal) in cultured cells. In fasting animals, autophagic degradation is induced in liver and other tissues.

We have identified and partially characterized an intracellular compartment where post-endoplasmic reticulum degradation of apolipoprotein B and lipid and

lipoprotein particles occurs. Characteristics of this compartment identified by us are as follows:

1. The proximal-most, distinct compartment of this autophagic pathway is a collection of vacuoles (Golgi-associated vacuoles, GAV) near the trans-Golgi

2. The GAV are encased by cisternal membranes which appear to be continuous with ribosylated endoplasmic reticulum. These membranes resemble "isolation membranes" involved with initial sequestration of cargo to be autophagocytosed.

3. The GAV contains five type of electron-dense particles, proposed to represent different maturational intermediates of lipid donor and and lipid acceptor particles. The same five types of particles are also seen within the secretory pathway (ie. the endoplasmic reticulum and the Golgi) but they show a different particle-particle and particle-membrane association.

4. Based on immunofluorescent studies, we deduced that Map1LC3 (marker of all autophagic structures, but most strongly of early autophagocytic structures) and apolipoprotein B (protein component of very low density lipoproteins) co-localize in the the GAV.

5. We have detected dense vacuolar structures, with a more advanced degradative content which are reactive for the autofluorescent drug monodansylcadaverine, near the GAV.

The invention will now be described by way of example; however the invention is not limited by the examples.

EXPERIMENTAL PROCEDURES

Materials Glycerol [^{14}C]trioleate (57 mCi/mmol), [^{3}H]glycerol (1.1 Ci/mmol), [^{14}C]oleic acid (55 mCi/mmol), [^{35}S]methionine/cysteine (1000 Ci/mmol), Protein A Sepharose™ CL-4B beads, and HRP-linked anti-mouse or anti-rabbit IgG antibodies were purchased from Amersham Pharmacia Biotech. [^{3}H]Eicosapentaenoic acid (150 Ci/mmol) was purchased from American Radiolabeled Chemicals, Inc. Fibronectin, monodansylcadaverine and oleic acid were obtained from Sigma. Triglyceride, and phospholipid standards were from Avanti Polar Lipids. Eicosapentaenoic acid (peroxide free) was from Cayman. Monoclonal anti-human apoB antibody 1D1 was a gift of R.

Milne and Y. Marcel (University of Ottawa Heart Institute). Polyclonal anti-MTP and anti-rat apoAI antisera were gifts of C. C. Shoulders (Hammersmith Hospital, United Kingdom) and J.E Vance (University of Alberta, Canada), respectively. The anti-rat Map1LC3 antiserum was kindly provided by A. Nara and T. Yoshimori (National Institute of Genetics, Mishima, Japan). Polyclonal antiserum against human LDL was produced in our laboratory. Protease inhibitor cocktail and chemiluminescent blotting substrate were purchased from Roche Diagnostics. Culture plate inserts (0.4 μm MILLICELL™-CM, 30-mm diameter) were purchased from Millipore.

Cell Culture and Fatty Acid Treatments Transfected McA-RH7777 cells stably expressing human apoB100 (McLeod et al., 1994, *J.Biol.Chem.* **269,** 2852-2862) were cultured in Dulbecco's modified Eagle's medium (DMEM) containing 10% fetal bovine serum (FBS), 10% horse serum and 200 μg/ml G418. Routinely, the cells were incubated with 0.4 mM fatty acids for 16-18 h in the presence of 20% FBS prior to experiments. During experiments, the cells were kept in fresh medium containing 20% FBS plus other reagents as indicated in the figure legends.

Pulse-chase Experiments In pulse-chase experiments where secretion efficiency of apoB was determined, cells were cultured in 60-mm dishes to 80% confluency, and preincubated with 0.4 mM oleate or EPA for 16 h. The cells were labeled with $[^{35}S]$methionine/cysteine (100 μCi/ml in 1 ml methionine- and cysteine-free DMEM containing 20% FBS and 0.4 mM oleate or EPA) for 1 h and incubated with chase medium (DMEM containing 20% FBS and 0.4 mM oleate or EPA) for indicated times. ^{35}S-apoB100 secreted in the medium and associated with the cells was immunoprecipitated using polyclonal antiserum raised against human LDL and resolved by SDS-PAGE/fluorography as described (Tran et al., 2000). In pulse-chase experiments where apoB100 in the membrane and lumenal content of different subcellular fractions was determined, cells in 100-mm dishes were labeled with $[^{35}S]$methionine/cysteine (200 μCi/ml in 4 ml methionine- and cysteine-free DMEM containing 20% FBS and 0.4 mM oleate or EPA) for 20 min. The cells were then incubated with chase medium for 15, 30 and 45 min. At the end of each chase time, the medium was collected and subjected to cumulative rate flotation centrifugation (Wang et al., 1999) to resolve apoB100-VLDL$_1$ (S_f > 100) and apoB100-VLDL$_2$ (S_f 20-100) from

other lipoproteins (*i.e.* IDL, LDL and HDL). The ^{35}S-apoB100 in each fraction was recovered by immunoprecipitation. Also, at the end of each chase time, the radiolabeled cells were harvested in 2 ml of ice-cold homogenization buffer (10 mM Tris-HCl, pH 7.4, 250 mM sucrose, 5 mM EDTA, and serine/cysteine protease inhibitor mixture), mixed with two 100-mm dishes of unlabeled cells, homogenized by passing ten times through a ball-bearing homogenizer, and subjected to subcellular fractionation and carbonate-treatment as described below.

Subcellular Fractionation Three subcellular fractions (*i.e.*, ER, fractions 1 through 3; *cis*/medial Golgi, fractions 4 through 8; distal Golgi, fractions 9 through 15) were obtained from the cell lysates using Nycodenz gradient centrifugation (Hammond and Helenius, 1994, *J.Cell Biol.* **126,** 41-52; Rickwood et al., 1982, *Anal.Biochem.* **123,** 23-31) of the post-nuclear supernatant as previously described (Tran et al., 2002).

Analysis of ApoB100 Associated with Membranes and Lumenal Contents of Microsomes Lumenal contents were separated from membranes by sodium carbonate treatment followed by centrifugation (Tran et al., 2002). The ^{35}S-labeled apoB100 proteins associated with the membrane and lumen were recovered by immunoprecipitation and analyzed by SDS-PAGE/fluorography as previously described (Tran et al., 2002).

Competitive Enzyme Linked Immunosorbent Assay (ELISA) – The ELISA plates were coated with human LDL (1 mg/ml in PBS, 16 h, 4°C), blocked with skim milk (5% in PBS, 2 h, 37°C), and washed three times with PBS containing 0.02% Tween-20. The plates were incubated with apoB monoclonal antibody 1D1 (1:64,000, 16 h, 4°C) in the presence of serial diluted concentrations of human LDL or medium samples. The plates were washed and incubated with horseradish peroxidase-linked anti-mouse IgG antibody (1:10,000, 2 h, 37°C), followed by addition of the liquid substrate system for ELISA (3,3',5,5'-tetramethyl-benzidine). The reaction was quantified colorimetrically by spectrophotometer reading at OD_{665}.

Transmission Electron Microscopy – Cells were cultured in normal culture medium on MILLICELL™-CM insert membranes precoated with fibronectin for 20 h, and incubated for additional 4 h with fresh DMEM containing 20% FBS and 0.4 mM oleate or EPA. The samples were processed for transmission electron microscopy as previously

described (Tran et al., 2002). Single and serial thin sections (silver-gold interference colors) were visualized in a Hitachi H-7000 transmission electron microscope, and captured at a range of negative magnifications (8,000-120,000 times). Panoramic tiling was used to capture large fields. The 3D model was prepared from Golgi fields from 7 consecutive serial images (positive magnification = 70,000 times), by the method previously described (Thorne-Tjomsland et al., 1998, *Anat.Rec.* **250,** 381-396), with the following modifications. The serial fields were scanned into Adobe Photoshop 5.5 of an Imac 700MHz G4 computer. Alignment of consecutive sections by fiducial markers was carried out prior to object-contouring and -separation. Concatenation and volume rendering were done in Synu on an SGI-OS 2, and image capture was with Photoshop on a Macintosh platform. The diameter of electron-dense particles, which represent a combination of lipoprotein particles and lipid droplets, were measured in 40 randomly selected Golgi regions from EPA-treated cells. Negative magnification was 40,000 times and positives were further magnified three times. Measurements were from positives, using a digital caliper [technical specifications in required range (0-150mm on positive): max resolution=0.01mm; accuracy=0.02mm; repeatability=0.01mm]. The precision in our system was tested by measuring the diameters of each of two electron-dense particles (20nm and 40nm diameter) 40 times; SD for the average converted measurements was ≤1nm. Criteria for selecting Golgi, establishing *cis-trans* polarity, and measuring lipid/lipoprotein particles were as described (Tran et al., 2002). Lipid/lipoprotein particles were classified as membrane-associated if directly apposed to the lumenal Golgi leaflet or with a membrane diverging from this, otherwise as lumenal.

Immunocytochemistry – Cells were plated onto fibronectin-precoated coverslips for 24 h, incubated with 0.4 mM oleate or EPA in DMEM containing 20% FBS for 4 h and fixed with 3% paraformaldehyde in PBS. Cells were permeabilized with 1% Triton X-100 in blocking buffer (10% FBS in PBS) for 30 min and probed with primary antibodies, *i.e.*, monoclonal antibody 1D1 (1:1000) for human apoB and polyclonal antibody against rat Map1LC3 (1:200) for 1 h. Cells were then incubated with a mixture of secondary antibodies (1:200), *i.e.*, of goat anti-mouse IgG conjugated with Alexa Fluor™488 (green) and goat anti-rabbit IgG conjugated with Alexa Fluor™594 (red) for 1 h. The coverslips were mounted onto glass slides using SlowFade AntiFade kits (Molecular

Probes) and the images were captured by an MRC-1024 laser scanning confocal imaging system.

Monodansylcadaverine (MDC) Labeling – Cells were plated onto poly-d-lysine coated glass bottom microwell dishes (MatTek Co) for 24 h and incubated with 0.4 mM oleate or EPA in DMEM containing 20% serum for 4 h. Cells were then incubated with 0.05 mM MDC in DMEM at 37°C for 10 min (Biederbick, 1995, *Eur.J.Cell Biol.* **66,** 3-14; Munafo and Colombo, 2001, *J.Cell Sci.* **114,** 3619-3629). After incubation, cells were washed three times with PBS and fixed in 3% paraformaldehyde for 30 min. After fixation, cells were washed four times with PBS and analyzed by fluorescence microscopy using an Olympus IX70 inverted microscope equipped with a 12 bit IMAGO SVGA CCD camera and the Till Polychrome IV monochrometer. MDC was exited at 380 nm using a fura filter set (T.I.L.L. Photonics GmbH). The images were processed using the TillVisION software, version 4.0.

Tandem Mass Spectrometry – Cells were kept in DMEM (20% FBS ± 0.4 mM oleate or EPA) for 16 h and re-incubated with fresh medium (20% FBS ± 0.4 mM oleate or EPA) for an additional 2 h. The membrane and lumen preparations from ER (Nycodenz fractions 1 through 3), *cis*/medial Golgi (fractions 4 through 8), and distal Golgi (fractions 9 through 15) were derived from cells pooled from eight 100-mm dishes. Lipids were extracted from the samples with chloroform/methanol/acetic acid/saturated NaCl/H_2O (4:2:0.1:1:2, by volume) in the presence of 230 pmol dimirystoyl (14:0-14:0) PC and 110 pmol dipalmitoyl (16:0-16:0) PE as internal standards. Aliquots of lipid extracts were applied to tandem mass spectrometry, and the molecular species (*i.e.* fatty acid composition) of PC and PE was determined by daughter ion analysis in the negative ion mode as previously described (Tran et al., 2002; DeLong et al., 1999, *J.Biol.Chem.* **274,** 29683-29688). The integrated area under the peak of each molecular species was quantified by comparing with those of internal standards.

Other Assays – The TG transfer activity of MTP was determined according to published method (Wetterau et al., 1992, *Science* **258,** 999-1001) with modifications (Wang et al., 1999). The phosphatidate phosphohydrolase activity was determined by an established method (Jamal et al., 1991, *J.Biol.Chem.* **266,** 2988-2996). Lipid extraction and analysis by TLC was performed as previously described (Tran et al.,

2000). Protein was determined using the BCA™ protein assay kit (Pierce).

RESULTS

EPA Treatment Inhibited Second-step Assembly of VLDL – Previous studies with man (Fisher et al., 1998, *J.Lipid Res.* **39,** 388-401; Hsu et al., 2000, *Am.J.Clin.Nutr.* **71,** 28-35; Sullivan et al., 1986, *Atherosclerosis* **61,** 129-134) and monkeys (Parks et al., 1989, *J.Lipid Res.* **30,** 1535-1544) have shown that EPA treatment results in reduction in the plasma TG concentration but has little effect on the amount of total circulating apoB100, which suggest an impairment in the incorporation of TG into VLDL during the second-step assembly (Parks et al., 1990, *J.Lipid Res.* **31,** 455-466). Using McA-RH7777 cells that stably expressed human apoB100, we analyzed the effect of EPA treatment on VLDL assembly and secretion. Analysis of the density distribution of apoB100 associated with lipoproteins in the medium (Fig. 1*A*) and microsomal lumen (Fig. 1*B*) showed marked reduction (by 50%) of ^{35}S-apoB100 in VLDL$_1$ (R_f > 100) and VLDL$_2$ (R_f 20-100) fractions in the medium at the end of 1-h chase in EPA-treated cells as compared with oleate-treated cells. Synthesis of apoB100 (determined by 5-20 min of labeling with [^{35}S]methionine/cysteine) between oleate- and EPA-treated cells was comparable (data not shown). Metabolic labeling of lipids with [^{3}H]glycerol showed 50% reduction in secretion of [^{3}H]glycerol-labeled TG from EPA-treated cells (Table I). Incorporation of [^{3}H]glycerol into cellular TG was comparable between oleate- and EPA-treated cells. Secretion of [^{3}H]glycerol-labeled PC was identical between oleate- and EPA-treated cells (Table I).

The amount of ^{35}S-apoB100 associated with particles of high density (*e.g.* IDL and LDL) was increased (by 6-fold) in the microsomal lumen of EPA-treated cells (Fig. 1*A* & *B*). The amount of total ^{35}S-apoB100 secreted from EPA-treated cells at the end of 1-h chase was comparable to that from oleate-treated cells (Fig. 1*A*). Additional pulse-chase experiments showed that the secretion efficiency of apoB100 from EPA-treated cells was 20% lower than from oleate-treated cells at the end of 3-h chase (Fig. 1*C*). There was also a slight decrease in the percentage of cell-associated ^{35}S-apoB100 in the EPA-treated cells at the end of 3-h chase. The reduced secretion efficiency of apoB100 in EPA-treated cells was mainly derived from the higher cellular [^{35}S]apoB100

(9.43×10^4 cpm/dish) after 1-h pulse than that of oleate-treated cells (6.40×10^4 cpm/dish), suggesting a protection in co-translational degradation and/or transient cellular accumulation of newly synthesized apoB. [Secretion efficiency of apoA-I was unaffected by EPA treatment (Fig. 1*C*)]. Quantification of apoB100 proteins using competitive ELISA also showed that the amount of apoB100 protein accumulated in the medium after 16-h incubation was not significantly different between oleate- and EPA-treated cells (oleate, 2.74 ± 0.48; EPA, 2.55 ± 0.43 □g/ml; n=3, $p > 0.05$). These results indicate that under conditions where synthesis of TG and apoB100 was relatively unaffected, EPA treatment resulted in marked reduction in the incorporation of TG into apoB100-containing lipoproteins but marginal reduction in the amount of total apoB100. EPA treatment did not affect the activity of MTP or phosphatidate phosphohydrolase (the key enzyme in TG synthesis) (data not shown).

The inability of EPA-treated cells to form VLDL in the face of normal apoB100 and TG synthesis suggested an impaired second-step VLDL assembly. Previous studies have shown that second-step assembly is achieved approximately 20 min after apoB100 translation in the Golgi apparatus in the presence of exogenous oleate (Tran et al., 2002). To gain insight into the impairment of VLDL assembly in EPA-treated cells, we monitored intracellular trafficking of apoB100 by pulse-chase experiments in conjunction with subcellular fractionation. The rates of ER exit and *cis*/medial Golgi transit of membrane-associated ^{35}S-apoB100 between oleate- and EPA-treated cells were comparable (Fig. 2*A*, *top* two panels), but the fraction of ^{35}S-apoB100 associated with distal Golgi membrane was markedly increased in EPA-treated cells (Fig. 2*A*, *bottom* panel). Since the membrane-associated apoB100 has been suggested to be the precursor of VLDL (Tran et al., 2002), augmented ^{35}S-apoB100 on the membrane may be indicative of impaired VLDL maturation within the distal Golgi. At the end of 45-min chase, there was a pronounced accumulation of ^{35}S-apoB100 in the distal Golgi lumen of EPA-treated cells, and the majority of ^{35}S-apoB100 was associated with IDL/LDL fractions (Fig. 2*B*). These results together indicate that assembly of TG-rich VLDL is impaired in EPA-treated cells, coincided with the formation/accumulation of abnormal high-density particles in the distal Golgi.

EPA-treatment Enhanced Autophagy – The observed accumulation of apoB100

within distal Golgi suggests impairment in VLDL maturation in EPA-treated cells. Previous studies have shown that EPA treatment promotes apoB degradation by an unidentified post-ER mechanism that requires PI 3-kinase activity (Fisher et al., 2001). We postulated that accumulation of assembly incompetent lipid/lipoprotein particles might be associated with autophagy, a process mediated turnover of cellular macromolecules and organelles that is essential for cell survival under various conditions and is sensitive to PI 3-kinase inhibition (Mizushima et al., 2002, *Cell Struct.Funct.* **27,** 421-429). To test this hypothesis, we examined localization of Map1LC3, a marker mainly of early autophagocytic structures (*i.e.*, isolation membranes and autophagosomes) (Kabeya et al., 2000, *EMBO J.* **19,** 5720-5728) and apoB100 in cells treated with oleate or EPA. As compared with untreated controls, EPA- and oleate-treated cells both showed enhanced penetration of Map1LC3 staining into the apoB100-rich perinuclear area (Fig. 3). There was partial co-localization of Map1LC3 and apoB100 in both EPA- and oleate-treated cells (Fig. 3, *overlay*, *arrowheads* and *inserts*). Fluorescent microscopic analysis of monodansylcadaverine (MDC), a specific marker of autophagolysosomes (Biederbick, 1995, *Eur.J.Cell Biol.* **66,** 3-14), also showed increased intensity and pronounced enlargement of the MDC-labeled vacuolar structures in EPA-treated cells (Fig. 4*A*). Transmission electron microscopy (TEM) of EPA-treated cells showed that dense vacuolar structures near the Golgi apparatus were larger and more prominent in EPA-treated cells as compared with control or oleate-treated cells (Fig. 4*B*, *arrows*). The resemblance in their distribution to that of MDC-labeled structures (Fig. 4*A*) clearly indicated that, although it does exist in all treatment, autophagolysosome formation is more pronounced in EPA-treated cells. These results suggest that post-ER degradation of apoB may be mediated by an autophagic process.

To determine if autophagosomes contain lipid/lipoprotein particles, TEM was performed with the emphasis on the electron dense particles distributed along the Golgi saccules, TGN/SG and vacuoles. Detailed morphometric analysis revealed five types of particles present in the Golgi apparatus and vacuoles (Fig. 5). Type I particles had an electron dense core surrounded by a less electron dense "halo" characteristic of a proteinaceous coat resembling that of cytoplasmic lipid droplets (Blanchette-Mackie et al., 1995, *J.Lipid Res.* **36,** 1211-1226; Brasaemle et al., 1997, *J.Lipid Res.* **38,** 2249-

2263; Servetnick et al., 1995, *J.Biol.Chem.* **270,** 16970-16973). The size of Type I particles (~100 nm) was in the low end of the range of measured cytoplasmic lipid droplets (0.1-50 μm in diameter) and exceeded the diameter of VLDL particles (30-80 nm) (Shelness and Sellers, 2001, *Curr.Opin.Lipidol.* **12,** 151-157). Hence, Type I particle may correspond to lipid donors for VLDL assembly. Particles showing partial (Type II) or complete (Type III) depletion of the core (Fig. 5*D, top* panel) may represent lipid donor intermediates. The type of phospholipid monolayer membrane which has been located between the core and halo of cytoplasmic lipid droplets by cryo-electron microscopy (Tauchi-Sato et al., 2002, *J.Biol.Chem.* **277,** 44507-44512), was not readily resolvable in Type I particles, but was detected in Type II and III particles near porosities within the periphery of the core (Fig. 5*D, top* panel, *arrows*). The size difference of Type IV and V particles (Table III) corresponded to HDL- and VLDL-type particles, respectively (Shelness and Sellers, 2001). However, Type V particles on the average were larger (54.5 nm) than d < 1.006 g/ml VLDL-particles (46.1 nm) isolated from the lumen of Golgi of livers from choline-deficient rats (Verkade et al., 1993, *J.Biol.Chem.* **268,** 24990-24996). The relative proportion of Type I:II:III:IV:V particles in the Golgi (12%:4%:13%:5%:66%) and in vacuoles (12%:2%:11%:5%:70%) was similar. Unlike in the Golgi where particles typically appeared singly or in pairs (*i.e.*, one Type I, II or III-, with one Type IV or V-particle) (Fig. 5*A* & *B*), particles in vacuoles were often found in "rosettes" (*i.e.*, multiple Type IV- and/or V-particles surrounding a single Type I, II or III particle) (Fig. 5*D*, *E*). Furthermore, Type I-III and V particles were more membrane-associated in the Golgi than in vacuoles, whereas Type IV particles were more membrane-associated in vacuoles than in the TGN/SV (Table III). The morphometric data thus imply that lipid/lipoprotein particles, which are sequestered into the autophagic pathway, differ from those, which remain in the secretory pathway, in their organization relative to one another, and relative to the limiting membrane.

The ultrastructure of Golgi-associated vacuoles in EPA-treated cells was analyzed further (Fig. 6*A-C*). Small vacuoles (*small asterisks*, Fig. 6*A-C*) containing electron-dense lipid/lipoproteins particles heterogeneous in size and morphology as presented above (Fig. 5 & Table III) were enveloped in membranous cisternae (*dotted lines*) that showed continuity with ER that was partially attached by ribosomes (Fig. 6*A*,

arrowheads). The ER-derived cisternal membranes encasing the *trans*-Golgi-associated lipid/lipoprotein-containing vacuoles resemble "isolation membranes" which sequester cargo during the early phase of autophagocytosis (Mizushima et al., 2002). Maturation from autophagosomes to autophagolysosomes has been shown to require fusion with late endosomes and/ or lysosomes, which is compatible with our findings that some vacuoles had buds (Fig. 6*B*, *white arrows*) and/or invaginations that accommodated small vesicles/tubules (Fig. 6*B* & *C*, *white asterisks*). Larger vacuoles (Fig. 6*A* & *C*, *large asterisks*) containing a dense material and probably corresponding to the MDC-reactive mature autophagolysosomes were located further away from the Golgi apparatus. Apparent fusion profiles were seen between vacuoles of various maturational stages (Fig. 6*C*), including between particle-containing vacuoles and dense vacuoles that was in agreement with autophago(lyso)some maturation (Reggiori and Klionsky, 2002, *Eukaryot.Cell* **1**, 11-21). The 3D serial section model showed the organization of particle-filled vacuoles relative to the Golgi, TGN and secretory granules (Fig. 6*D*). It also provided evidence that vacuolization begins within the Golgi since several particle-filled dilations of *trans*-Golgi saccules (Fig. 6*E*, *light blue*) were encased by cisternal membranes (Fig. 6*E*, *white dotted lines*) continuous with those (Fig. 6E, *red*) which enveloped particle-filled vacuoles (Fig. 6*E*, *1-4). These data suggest the involvement of autophagosomes and autophagolysosomes in degradation of lipid/lipoproteins in EPA-treated cells, and that the autophagocytic process originates at the *trans*-Golgi compartment.

Alteration of Membrane Phospholipid Composition and Remodeling by Oleate and EPA – The interfaces between adjacent lipid/lipoprotein particles and between the lipid/lipoprotein particles and the Golgi/vacuolar limiting membrane are presumably defined by apposing phospholipid monolayers. Furthermore, data from our previous works (Tran et al., 2002) have suggested an important role of membrane phospholipid remodeling in VLDL assembly (Tran et al., 2000). Hence, to determine if the impaired VLDL assembly and the augmented post-ER degradation in the Golgi-associated vacuoles under EPA-treated conditions were associated with altered phospholipid metabolism, we first compared membrane phospholipid composition between control (*i.e.* incubated in DMEM containing 20% FBS), oleate-, and EPA-treated cells. The PC

mass associated with total intracellular microsomes was increased by 55% by oleate-treatment; most of the increase occurred in the ER (by 87%) and distal Golgi (by 77%) (Table II). In contrast, EPA treatment had a marginal effect on total PC mass, with a slight redistribution between distal and *cis/*medial Golgi. However, the effect of EPA treatment on microsome-associated PE was striking; total PE was nearly doubled with 175% increase in the distal Golgi alone. On the other hand, total PE was only marginally changed (increased by 27%) with oleate treatment. Overall, oleate treatment resulted in increased PC content in microsomal membranes throughout the entire secretory pathway (chiefly in ER and distal Golgi), whereas EPA treatment caused a massive increase in PE content thus bringing down the PC-to-PE ratio. Moreover, oleate treatment resulted in increase in PC species containing 18:1(n-9) acyl chain at either the *sn*-1 or *sn*-2 position (*i.e.*, 16:0-18:1, 18:1-18:1, 18:0-18:1, 18:1-20:1), of which the 18:1-18:1PC was the most abundant species in all subcellular compartments (Fig. 7*A*). In EPA-treated cells, all of the 18:1(n-9)-containing PC species were markedly reduced in the ER and Golgi membranes (Fig. 7*A*, *arrows*). The PC species increased upon EPA treatment were 16:0-20:5 and 18:0-20:5 that contained 20:5(n-3) in the *sn*-2 position, suggesting that incorporation of 20:5(n-3) into PC is mediated mainly through deacylation/reacylation mechanism. In the case of PE, EPA treatment resulted in marked elevation of 16:0-20:5, 18:2-20:5, 18:2-22:6 and 18:0-22:6 species in all subcellular compartments, with 18:2-22:6 being most abundant in the ER (Fig. 7*B*). Like what was seen in PC, EPA treatment also decreased PE species containing 18:1(n-9) acyl chain (*i.e.* 16:0-18:1, 18:1-18:2, 18:1-18:1, and 18:0-18:1) (Fig. 7*B*, *arrows*). However, the PE species containing 18:1(n-9) acyl chain were marginally increased in oleate-treated cells, indicating that 18:1(n-9) was preferentially incorporated into PC over PE. Taken together, phospholipid species analysis shows that EPA treatment not only decreases PC-to-PE ratio but also decreases PC and PE species containing 18:1(n-9) acyl chain. The effect of EPA treatment on PC-to-PE ratio resembles that of choline deficiency (Ridgway et al., 1989, *J.Biol.Chem.* **264**, 1203-1207), whereas the effect of lowering phospholipid species containing 18:1(n-9) acyl chain is reminiscent of $iPLA_2$ inhibition (Tran et al., 2000). In both choline deficiency and $iPLA_2$ inhibition situations, secretion of VLDL was inhibited but secretion of dense lipoproteins was not.

We next monitored remodeling of the membrane phospholipids and its relationship with TG synthesis and secretion. For this purpose, the cells were labeled with [^{14}C]oleate or [^{3}H]EPA for 2 h, and chased up to 4 h in the presence of unlabeled exogenous oleate or EPA, respectively. At the end of 2-h labeling, PC, PE, TG, and CE accounted for 53%, 8%, 27%, and 2%, respectively, of total ^{14}C-labeled cellular lipids in oleate-treated cells (Fig. 8*A-D*, *top*, at *0 h*), and 48%, 36%, 3%, and 0.1%, respectively in EPA-treated cells (Fig. 8*A-D*, *bottom,* at *0 h*). Thus, [^{14}C]oleate was incorporated mainly into PC and TG, while [^{3}H]EPA was incorporated mainly into PC and PE, and not into TG. During the chase, the counts of [^{14}C]oleate-labeled PC, PE and TG were relatively constant in the absence of exogenous oleate (Fig. 7*A-C*, *top*, *closed circles*), which indicates a low rate of turnover and agrees with our previous observation (Tran et al., 2000). In [^{3}H]EPA-labeled cells, the counts associated with PC was decreased with a concomitant increase in PE during the chase (Fig. 8*A-B*, *bottom*, *closed triangles*), indicating an active movement of 20:5(n-3) acyl chain from PC to PE through phospholipid remodeling under basal conditions (Balsinde, 2002, *Biochem.J.* **364,** 695-702). Inclusion of exogenous oleate during chase stimulated turnover of [^{14}C]oleate-labeled PC, and the decreased counts from PC were transferred to TG (Fig. 8*A-C, top*, *opened circles*). In [^{3}H]EPA-labeled cells, turnover of PC and PE were both stimulated by exogenous EPA, and the 20:5(n-3) acyl chain derived from PC and PE was incorporated into TG during chase. At the end of 4-h chase, ~30% of total [^{3}H]EPA radioactivity in the cells was associated with TG (Fig. 8*A-C*, *bottom*, *opened triangles*). Phospholipid remodeling induced by exogenous fatty acids was clearly indicated by the enhanced release of free [^{14}C]oleate and [^{3}H]EPA into the medium during chase (Fig. 9*D*, *opened circles & triangles*). These results suggest that during the process of phospholipid remodeling which is stimulated by exogenous fatty acids, the 18:1(n-9) and 20:5(n-3) acyl chains derived from respective phospholipid deacylation are utilized efficiently for TG synthesis. Incorporation of EPA into CE during chase was negligible (Fig. 8*D*, *bottom, opened triangles*), which agrees with the notion that EPA is a poor substrate of acyl-CoA:cholesterol acyltransferase (Rustan et al., 1988, *J.Biol.Chem.* **263,** 8126-8132).

A striking difference was observed between [^{14}C]oleate-TG and [^{3}H]EPA-TG

secretion. While TG species labeled with 18:1(n-9) acyl chain were secreted during chase and its secretion was further stimulated by exogenous oleate (Fig. 9*C*, *top*), TG species labeled with [^{3}H]EPA was poorly secreted regardless of the presence of exogenous EPA (Fig. 9*C*, *bottom*). These results together suggest that TG species containing 18:1(n-9) or 20:5(n-3) acyl chain have different metabolic fates; while 18:1(n-9)-TG is utilized for lipoprotein assembly/secretion, 20:5(n-3)-TG is not. Secretion of [^{3}H]EPA-PC and [^{14}C]oleate-PC was comparable, at least during initial chase times (Fig. 9*A*). Secretion of [^{3}H]EPA-PE was higher than that of [^{14}C]oleate-PE (Fig. 9*B*), whereas secretion of [^{14}C]oleate-CE was higher than that of [^{3}H]EPA-CE was low (Fig. 9*E*).

Intracellular Distribution of 18:1(n-9)- or 20:5(n-3)-labeled Lipids – The close relationship between 18:1(n-9)-PC and secreted 18:1(n-9)-TG and between 20:5(n-3)-PE and the poor lipoprotein substrate 20:5(n-3)-TG suggests that phospholipid turnover is intimately associated with the TG substrate availability for VLDL assembly/secretion. We hypothesized that the asymmetric distribution of PC and PE on the microsomal membranes (*i.e.* PC enriched on the lumenal side whereas PE on the cytosolic side), together with the alteration of the PC-to-PE ratio upon different fatty acid treatment, might contribute to the partition of different TG species between the storage pool (in cytosol) and lipoprotein assembly pool (in the microsomal lumen). To test this hypothesis, we pulse-labeled the cells for 2 h and then determined intracellular distribution [^{14}C]oleate- or [^{3}H]EPA-labeled lipids at the end of 4-h chase in the presence or absence of corresponding exogenous fatty acids (Fig. 10). At the end of chase, [^{14}C]oleate was mainly associated with membrane PC, whereas [^{3}H]EPA was mainly associated with membrane PE (Fig. 10*A* & *B*, *microsomal membranes*, *nuclei/mitochondria*, *opened bars* of PC and PE). Addition of exogenous oleate or EPA during chase resulted in the release of [^{14}C]oleate or [^{3}H]EPA from respectively labeled phospholipids (Fig. 10*A* & *B*, *microsomal membranes*, *nuclei/mitochondria*, differences between *opened* and *solid bars* of *PC* and *PE*), and a subsequent incorporation of [^{14}C]oleate or [^{3}H]EPA into TG in the cytosol (Fig. 10*A* & *B*, *cytosol*, differences between *opened* and *solid bars* of *TG*). Cytosolic 18:1(n-9)-TG was increased by 2-fold in cells chased with exogenous oleate (Fig. 10*A*, *cytosol*, compare *solid* and *opened bars* of *TG*). More strikingly, cytosolic 20:5(n-3)-TG was increased by almost 8-fold when cells

were chased with exogenous EPA (Fig. 10*B*, *cytosol*, compare *solid* and *opened bars* of *TG*). In a separate experiment where cells were pulse-labeled with [^{3}H]glycerol and then chased in the presence of either oleate or EPA, the increase in cytosolic [^{3}H]glycerol-TG was also more pronounced in EPA-treated cells than in oleate-treated cells (data not shown). These results together with the TEM data (Fig. 4*B*, note label L for lipid droplets on the TEM images) indicate that 20:5(n-3)-TG, in comparison to 18:1(n-9)-TG, is diverted more into cytosolic storage pools. Both [^{3}H]EPA-TG and [^{14}C]oleate-TG were detectable at comparable levels in the microsomal lumen (Fig. 10*A* & *B*, *microsomal lumen*). However, as shown in Fig. 9*C*, the [^{3}H]EPA-TG was poorly secreted as compared with [^{14}C]oleate-TG (Fig. 10*A* & *B*, *medium*).

DISCUSSION

Differential remodeling of membrane phospholipid induced by oleate and EPA impacts the second-step VLDL assembly in McA-RH7777 cells – The current study has demonstrated that the second-step assembly of VLDL is regulated by membrane phospholipid remodeling (*i.e*, deacylation/reacylation) under the influx of exogenous fatty acids. One of the important functional aspects of phospholipid remodeling in relation to VLDL assembly is the utilization of released acyl chain (upon deacylation) in the synthesis of TG. The preferential incorporation of oleate into membrane PC (Fig. 8*A*) is likely mediated by both the *de novo* and remodeling pathways, for its presence in both *sn*-1 and *sn*-2 position of the glycero-backbone of PC (Fig. 7*A*). In contrast, the preference incorporation of EPA into the *sn*-2 position of membrane phospholipids (Fig. 7*B*) and its subsequently transferred from PC to PE shown in our phospholipid remodeling assay (Fig. 8*A* & *B*) are clear indicator of remodeling process. The intrinsic nature of polyunsaturated fatty acid incorporation into phospholipids through deacylation/reacylation process mediated by intracellular Ca^{2+}-independent phospholipase A_2 and PE being the preferential destination pool for EPA incorporation have recently demonstrated in other cell types (Balsinde, 2002). Upon influx of exogenous fatty acids, both oleate and EPA released from phospholipid remodeling are utilized for TG synthesis with little selectivity (Fig. 8*C*). However, 20:5-containing TG was poorly secreted as compared with 18:1-containing TG (Fig. 9), suggesting that

20:5-TG is inefficiently utilized for VLDL assembly. The TG-lowering effect of EPA therefore can not be explained by its inhibition of key enzymes in TG synthesis such as phosphatidate phosphohydrolase (Wong and Marsh, 1988, *Metabolism* **37,** 1177-1181) and diacylglycerol acyltransferase (Berge et al., 1999, *Biochem.J.* **343 Pt 1,** 191-197). The normal phosphatidate phosphohydrolase assayed *in vitro* (data not shown) and the comparable incorporation of [^{3}H]glycerol into cell-associated TG in oleate- and EPA-treated cells in present study (Table I) and in others (Lang and Davis, 1990) ruled out that TG-lowering effect of EPA is caused by defects in TG synthesis. Reduction in VLDL-TG secretion is also not caused by impairment of the first-step assembly, since EPA treatment resulted in normal apoB synthesis and ER exit as compared to oleate treatment. In fact, EPA may protect co-translational degradation of apoB as revealed by increased number of apoB molecules that exit the ER and accumulate in the distal Golgi (Fig. 2). The marginal reduction of the total apoB secreted in the medium from EPA treatment as compared to oleate is in accord with the *in vivo* observation that fish oil has little effect on plasma apoB but markedly decreases plasma TG in humans (Fisher et al., 1998; Hsu et al., 2000). The presence of elevated buoyant dense apoB-containing particles and/or LDL-apoB concentrations in humans ingesting fish oil (Hsu et al., 2000; Sullivan et al., 1986) is also reminiscent of impaired second-step assembly. Reduction in VLDL-TG secretion but not apoB has also been observed in monkey liver perfusion studies; compared to lard-fed controls, fish oil-fed monkeys secreted the same number of VLDL particles with lower TG and cholesterol ester content (Parks et al., 1989; Parks et al., 1990). Thus, the current data revealed that the intrinsic nature of membrane phospholipid deacylation/reacylation and the differential incorporation of oleate and EPA into PC and PE lead to the formation of different TG pools that may or may not be accessible and efficiently utilized in the second-step assembly.

Alteration of membrane PC-to-PE ratio is associated with an accumulation of TG in the cytosolic pool and activation of post-ER degradation – In addition to the importance of PC and PE remodeling in the formation of different TG species (*i.e.*, 18:1-TG versus 20:5-TG), the current study also shows that a decrease in the PC-to-PE ratio within the microsomal membrane is associated with impaired second-step VLDL assembly and accumulation of TG in the cytosolic pool. Alteration of PC-to-PE ratio

could be attained by changing of either PC or PE content in the microsomal membranes and may be an indicator for the efficiency of the second-step VLDL assembly. Although the nature of these changes is not totally clear, our previous (Tran et al., 2000) and current data (Table II) indicate that oleate treatment of McA-RH7777 cells increased PC content in the microsomal membranes(Wang et al., 1999), particularly in the ER and distal Golgi. In contrast, EPA treatment resulted in an increase in PE content (thus lowering PC-to-PE ratio) in the membrane of distal Golgi (Table II) that was effectively preventing VLDL assembly. An increase in liver PE levels has also been reported in EPA-fed rats (Kotkat et al., 1999, *Comp Biochem.Physiol A Mol.Integr.Physiol* **122,** 283-289). Lowering PC-to-PE ratio of liver microsomal membranes that is associated with impaired second-step VLDL assembly (decreased VLDL secretion but not HDL secretion) has been observed in other models such as choline deficiency (Ridgway et al., 1989) and inhibition of PE methylation pathway (Nishimaki-Mogami et al., 2002);(Noga et al., 2002, *J.Biol.Chem.* **277,** 42358-42365). Disruption of PE to PC conversion via the PE methylation pathway by chemical inhibition (Nishimaki-Mogami et al., 2002)or by genetic disruption of PE methyltransferase in mice (Noga et al., 2002) showed reduction of PC-to-PE ratio that was associated with impaired apoB100-VLDL secretion. In PE methyltransferase deficient animals, particularly in males, the increased in liver PE was associated with liver TG accumulation and decreased plasma TG. Unlike primary rat hepatocytes, McA-RH7777 cells lack PE methyltransferase activity (Cui et al., 1995, *Biochem.J.* **312,** 939-945) and are unable to assemble VLDL unless exogenous oleate is supplemented to the medium. The restoration of VLDL assembly in McA-RH7777 cells in the presence of exogenous oleate may in part be resulted from re-establishing of PC-to-PE ratio (due to elevation of PC content) permissive for VLDL assembly. Reconstitution of PE methyltransferase activity in McA-RH7777 cells increased secretion of TG in apoB100-VLDL (DeLong et al., 1999) and generated diverse PC species which resembled those synthesized by the methylation pathway in hepatocytes (Noga et al., 2002). The asymmetric distribution of membrane phospholipids (Daleke, 2003, *J.Lipid Res.* **44,** 233-242) (*i.e*, PC enriched in the lumenal leaflet and PE enriched in the cytosolic leaflet of the microsomal membranes, particularly at the site of VLDL assembly, the Golgi) together with their intrinsic property

of accepting and donating different fatty acyl chains during remodeling, contribute to the formation of two metabolically distinct TG pools. As a result, TG formed in EPA treatment was accumulated more in the cytosolic pool (Figs. 4*B* & 10) that might be inaccessible for VLDL assembly. Taken together, we propose that phospholipid remodeling together with the alteration of PC-to-PE ratio induced by different fatty acid treatments have strong impact TG synthesis/distribution and VLDL assembly.

Could the altered PC-to-PE ratio in the membrane of distal Golgi also be involved in the post-ER degradation? One of the essential proteins involved in the entire process of autophagosome formation is Map1LC3, which exists in two forms: an 18 kDa cytosolic form and a 16 kDa autophagosome membrane-associated form (Kabeya et al., 2000). The yeast homolog Apg8/Aut7p is conjugated to PE when binding to the autophagosome membrane; hence, the membrane-bound Map1LC3 has been postulated as a PE-conjugated form (Ichimura et al., 2000, *Nature* **408,** 488-492). If this is the case, then the decreased ratio of PC to PE in microsomal membranes, particularly in the distal Golgi may contribute to initiating the autophagocytic process, observed near the *trans*-Golgi (Fig. 6). Autophagosome formation begins with formation of a membrane structure termed an "isolation membranes", postulated to be derived from the ER (Ueno et al., 1991, *J.Biol.Chem.* **266,** 18995-18999), the *trans*-Golgi network (Yamamoto et al., 1990, *J.Histochem.Cytochem.* **38,** 573-580), and/or a unique, uncharacterized intracellular compartment (Stromhaug et al., 1998, *Biochem.J.* **335,** 217-224), that progressively enwraps the cargo. Fusion between the isolation membrane and the vacuolar membrane leads to formation of autophagosome, which in turn fuses with lysosomes (Yamamoto et al., 1990) to form autophagolysosomes, resulting in degradation of the lumenal contents. The detection by TEM of lipid/lipoprotein-containing vacuoles encased in a double membrane structure near the *trans*-Golgi (Fig. 6), and the increased punctate staining of the autophagocytic markers Map1LC3 and MDC by confocal and fluorescent microscopy (Figs. 3 & 4), respectively, clearly indicate that autophagy is induced by EPA treatment. Although the constitutive nature of autophagosome formation is essential for cell survival (Klionsky and Emr, 2000, *Science* **290,** 1717-1721), as it was also detected in both oleate-treated and control cells, the increased autophagy in EPA treatment (Fig. 4*A* & *B*) may play a role in

the disposal of accumulated aberrant lipid/lipoproteins in the distal Golgi and/or lipid particles in the cytosol as a result of impairment of second-step assembly. Autophagosome formation in cultured cells can be stimulated by starvation condition (Klionsky and Emr, 2000) or inhibited by wortmannin or 3-methyladenine, inhibitors of phosphatidylinositide 3-kinase (Mizushima et al., 2001, *J.Cell Biol.* **152,** 657-668). In light of the evidence that the non-proteosomal degradation of apoB is sensitive to phosphatidylinositide 3-kinase inhibition (Fisher et al., 2001; Phung et al., 1997), our current data suggests that autophagy represents a missing link for post-ER degradation in VLDL assembly. Thus, while apoB degradation during first-step assembly is known to be mediated by the ubiquitin-proteasome pathway (Fisher and Ginsberg, 2002; Yao et al., 1997), we propose that aberrant lipid/lipoproteins generated from impaired second-step assembly are removed at least in part by autophagy. The relationship between phospholipid remodeling and distribution of metabolically distinct TG pools as well as the autophagosome formation is depicted in Fig. 11.

How can post-ER degradation occur with marginal change in total secreted apoB, under the current experimental conditions? The most feasible explanation supported by our current data is that EPA may protect co-translational degradation of apoB resulting in an increase in the number of apoB molecules, which exit the ER and accumulate in the Golgi (Fig. 2). At the distal Golgi, a subset of apoB involved in the formation of TG-rich VLDL may be subjected to autophagic degradation, as shown by partial co-localization of Map1LC3 and apoB (Fig. 3). However, since the number of apoB molecules in $VLDL_1$ fraction ($S_f > 100$) is about 10-20% of total apoB that carries most of the secreted TG (Wang et al., 1999), the post-ER degradation of apoB in this fraction, though leading to a significant reduction of secreted TG, may therefore result with no detectable change in total secreted apoB.

The importance of membrane lipids containing 18:1(n-9) and 20:5(n-3) acyl chain in VLDL assembly – Although compartmentalized 18:1(n-9)-TG and 20:5(n-3)-TG pools may explain the difference in how oleate- and EPA-treatment affect second-step assembly, it is also possible that alterations in membrane phospholipid species directly impact VLDL assembly. The molecular species analysis clearly shows that EPA treatment results in marked reduction of membrane-associated PC and PE species

containing 18:1(n-9) and in an increase of species containing 20:5(n-3) (Fig. 7*A* & *B*). We have demonstrated previously that in McA-RH7777 cells, reduction of 18:1(n-9) acyl chain in membrane PC and PE, either by oleate deprivation (McLeod et al., 1996) or by inhibition of $iPLA_2$ (Tran et al., 2000), is closely associated with impaired second-step VLDL assembly. Both studies suggest that oleate does not merely serve as a substrate for the TG synthesis, which precedes or coincides with VLDL assembly. Rather, incorporation of 18:1(n-9) acyl chain into microsomal phospholipids may establish a membrane platform for efficient bulk incorporation of TG into VLDL. Establishing a membrane milieu compatible with second-step assembly is important, especially in view of a large body of evidence that membrane-associated apoB100 within microsomes is the precursor of assembled/secreted VLDL(Tran et al., 2002; Stillemark et al., 2000; Hebbachi and Gibbons, 2001, *J.Lipid Res.* **42,** 1609-1617; Rustaeus et al., 1998, *J.Biol.Chem* **273,** 5196-5203). In this context, the presence of other 18:1(n-9)-containing lipids such as phosphatidic acid and diglyceride which are important for membrane dynamics (Antonny et al., 1997; Chernomordik et al., 1995) may also facilitate the second-step assembly process.

The massive accumulation of PE in the Golgi apparatus accompanied with markedly depleted 18:1(n-9)-containing PC in EPA-treated cells appears to reveal for the first time the assembly intermediates of lipid donors and acceptors at the VLDL assembly site. Our TEM morphometric analysis data of EPA treated cells showed different types of lipid/lipoprotein particles, at the distal Golgi and vacuolar structures, resembling of original lipid donors (Type I), intermediate lipid donors (Types II and III) and nascent lipoproteins (Types IV and V). As membrane associated apoB100 being precursors of VLDL, the impaired second-step assembly was clearly manifested by accumulation of apoB100 in the membrane of distal Golgi (Fig. 2*A*) and the formation of degradation vacuoles housing intermediate lipid/lipoprotein particles (Fig. 5). These observations were not possible to obtain with oleate treatment, for the transient appearance and rapid release of VLDL right after its formation (Tran et al., 2002). The current study therefore demonstrates that tipping towards one side or the other of the balance between post-ER degradation and second-step VLDL assembly can be influenced by alteration of membrane phospholipid species.

Of the multiple effects of EPA treatment (Jump, 2002, *J.Biol.Chem.* **277,** 8755-8758), changes in phospholipid composition and species have recently drawn attention. EPA is shown to influence the composition of membrane lipid rafts and their association with acylated proteins (Stulnig et al., 2001, *J.Biol.Chem.* **276,** 37335-37340). Human apoB100 is known to be a palmitoylated protein, although the role of apoB100 palmitoylation in VLDL assembly/secretion is unclear (Vukmirica et al., 2003, *J.Biol.Chem.* **278,** 14153-14161; Zhao et al., 2000, *Mol.Biol.Cell* **11,** 721-734). Potential palmitoylation sites within human apoB100 might be acylated by EPA; such promiscuous S-acylation has been found in other proteins (Liang et al., 2001, *J.Biol.Chem.* **276,** 30987-30994). Thus, changes of lipid microdomains and/or S-acylation of proteins including apoB100 by EPA may play important role in the second-step assembly that merits further study.

The current study has revealed a new mechanism whereby EPA-treatment exerts TG-lowering effect, and emphasizes the close relationship between phospholipid metabolism (*i.e. de novo* biosynthesis, turnover, remodeling) and important cellular processes such as assembly, secretion and degradation of LpBs. A better understanding of the n-3 fatty acid actions will provide a rational nutraceutical approach to the prevention and treatment of dyslipidemia and atherosclerosis. While the preferred embodiments of the invention have been described above, it will be recognized and understood that various modifications may be made therein, and the appended claims are intended to cover all such modifications which may fall within the spirit and scope of the invention.

Table I

Incorporation and secretion of [^{3}H]glycerol-labeled TG and PC in cells treated with oleate or EPA

Cells pretreated (16 h) with oleate or EPA were metabolically labeled with [3H]glycerol for 2 h. Oleate or EPA was present during labeling. Lipids of cells and media were extracted, and [^{3}H]PC and [^{3}H]TG were resolved by TLC as described in "Experimental Procedures". Data were means ± SD of triplicate determination.

	TG		PC	
	Medium	Cell	Medium	Cell
		(cpm x 10^{-3})		
Oleate	12.87 ± 1.59	33.80 ± 0.62	4.10 ± 0.12	15.00 ± 0.23
EPA	7.18 ± 0.96*	40.84 ± 0.70	3.86 ± 0.57	15.80 ± 0.44

*, *$p < 0.05$, compared to medium TG of oleate treatment*

Table II

Changes of PC and PE contents in membranes of different subcellular compartments of oleate and EPA treated cells

The subcellular compartments of cells incubated with oleate or EPA were fractionated by Nycodenz gradient centrifugation, and the membranes of distal Golgi, *cis*/medial Golgi and ER were isolated by sodium carbonate treatment followed by ultracentrifugation. Total lipids were extracted and subjected to tandem mass spectrometry for the analysis of PC and PE as described in the "Experimental Procedures". The data were means ± SE of three separate experiments and expressed as percent change over the corresponding value of untreated control.

	oleate		EPA	
	PC	PE	PC	PE
	(% change over control)			
distal	77 ± 28*	7 ± 3	21 ± 15	175 ± 65**
cis/medial	26 ± 32	-20 ± 24	-30 ± 18	25 ± 31
ER	87 ± 34*	122 ± 47	8 ± 2	117 ± 11
Total	55 ± 7*	27 ± 1	-8 ± 6	88 ± 28**

**$p < 0.05$, compared to PC of EPA treatment*

***$p < 0.05$, compared to PE of oleate treatment*

Table III

Morphometric analysis of particles in the lumenal content of Golgi and Golgi-associated vacuoles in EPA-treated cells

	Golgi saccules					
	1	2	3	4-6	TGN/SV	GA-V
Type I						
Overall diameter (nm)	100 ± 15	78 ± 18	85 ± 11	77 ± 16	82 ± 15	78 ± 22
Core diameter (nm)	68 ± 22	56 ± 17	55± 14	57 ± 19	59 ± 16	57 ± 22
Membrane association (%)	100	84	80	73	56	33
Number of particles	8	19	15	22	9	27
Type II						
Overall diameter (nm)	90 ± 10	93 ± 13	96 ± 14	-	-	101 ± 20
Core diameter (nm)	55 ± 13	57 ± 20	49 ± 17	-	-	70 ± 29
Membrane association (%)	100	83	75	-	-	25
Number of particles	10	6	8	0	0	4
Type III						
Overall diameter (nm)	79 ± 10	67 ± 10	68 ± 11	62 ± 12	69 ± 16	62 ± 9
Core diameter (nm)	50 ± 13	37 ± 17	39 ± 15	32 ± 14	39 ± 14	32 ± 11
Membrane association (%)	100	83	83	82	73	46
Number of particles	5	12	23	28	15	24
Type IV			(1-3)			
Overall diameter (nm)			21 ± 3	20 ± 4	22 ± 1	19 ± 3
Membrane association (%)			67	50	20	45
Number of particles			18	10	5	11
Type V						
Overall diameter (nm)	51 ± 14	54 ± 16	56 ± 15	53 ± 14	52 ± 12	50 ± 13
Membrane association (%)	96	83	66	64	66	42
Number of particles	25	94	94	107	95	155

TGN: trans-Golgi network
SV: secretory vesicles
GA-V: Golgi-associated vacuoles
Details of the experiment was described under "Experimental Procedures"

CLAIMS

1. A method of inducing reducing serum levels of triglycerides and/or very low density lipoprotein comprising administering to an individual in need of such treatment an effective amount of an autophagolysosome inducing compound.

2. The method according to claim 1 wherein the individual suffers from or is at risk of developing at least one of the following: hypercholesterolemia, hyperlipidemia, hyperlipoproteinemia, atherosclerosis, cardiovascular disorders, coronary heart disease, coronary artery disease, or stroke.

3. The method according to claim 1 wherein the autophagolysosome inducing compound is selected from the group consisting of Map1LC3, GABARAP, GATE16 and Class III P13'kinase.

4. A pharmaceutical composition capable of inhibiting autophagocytosis selected from the group consisting of Wartmannin, 3 methyladenine, LY294002, Class I P13'kinase and rapamycin.

5. A pharmaceutical composition capable of inducing autophagocytosis selected from the group consisting of Map1LC3, GABARAP, GATE16 and Class III P13'kinase.

6. A method of identifying autophagolysosome modulating compounds comprising:

administering a test compound to cells in a cell culture system; and

assaying for VLDL and VLDL precursors in ER and Golgi fractions and in the culture medium,

wherein an abnormal value compared to untreated control cells indicates that the compound modulates autophagolysosome activity.

7. The method according to claim 6 wherein the cells in the cell culture system are cultured rat hepatocyte or rat hepatoma cells expressing human apoB100.

8. A method of identifying autophagolysosome modulating compounds comprising:

administering a test compound to cells in a cell culture system; and

detecting the degree of co-localization of apoB100 and Map1LC3 by immunofluoresence, wherein an abnormal value compared to untreated control cells

indicates that the compound modulates autophagolysosome activity.

ABSTRACT

Processing (*i.e.* assembly and degradation) of very low density lipoprotein (VLDL), and accompanying changes in membrane phospholipid remodeling, was studied in human apolipoprotein (apo) B100-transfected McA-RH7777 cells treated with oleic acid (oleate, 18:1(n-9)) or eicosapentaenoic acid (EPA, 20:5(n-3)). In EPA-treatment, when the synthesis of apoB100 and its ER exit were unaffected, there was increased association of apoB100 with membranes of the distal Golgi coupled with decreased incorporation of triglyceride (TG) into VLDL within the distal Golgi lumen, resulting in formation of primarily dense, TG-poor, apoB-containing lipoproteins. Lipoprotein/lipid particles similar to those seen in the Golgi, were also detected by transmission electron microscopy in *trans*-Golgi associated vacuoles; these were reactive with early autophagocytic marker Map1LC3 and showed partial co-localization with apoB. The later autophagic marker, monodansylcadaverine, was detected in associated degradative vacuoles, which were progressively larger in control, oleate- and EPA-treated cells. Lipid analysis revealed that 18:1(n-9) was preferentially incorporated into phosphatidylcholine (PC) while 20:5(n-3) into phosphatidylethanolamine (PE). In comparison to oleate, cells treated with EPA resulted in an increase in membrane PE, particularly at the distal Golgi, and thus lowering the PC-to-PE ratio. During phospholipid remodeling, both 18:1(n-9) derived from PC and 20:5(n-3) derived from PE were utilized equally for TG synthesis. However, 18:1(n-9)-TG was efficiently incorporated into VLDL for secretion whereas 20:5(n-3)-TG was a poor lipoprotein substrate. These results suggest that phospholipid remodeling has strong impact on the recruitment of TG during VLDL assembly and formation of an autophagic, post-ER degradative compartment.

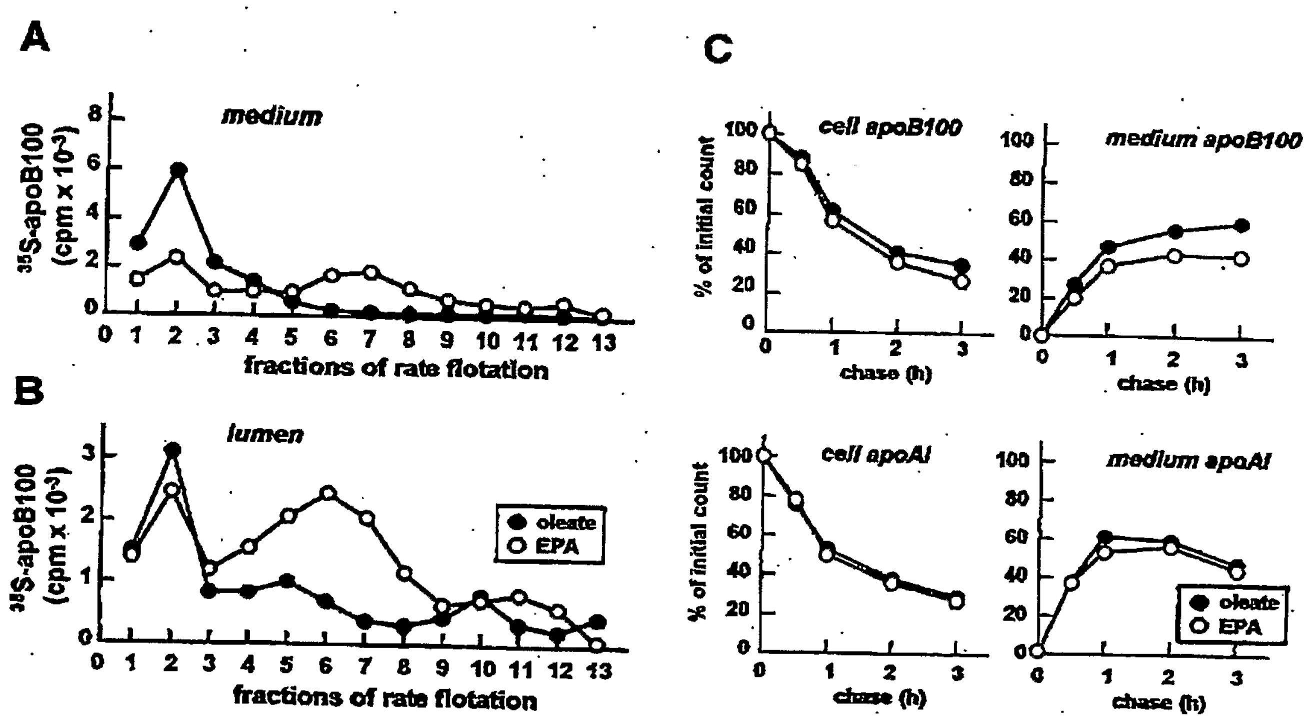
A
medium
^{35}S-apoB100 (cpm x 10^{-3})
fractions of rate flotation
B
lumen
^{35}S-apoB100 (cpm x 10^{-3})
fractions of rate flotation
oleate
EPA
C
cell apoB100
medium apoB100
% of initial count
chase (h)
cell apoAI
medium apoAI
% of initial count
chase (h)
oleate
EPA

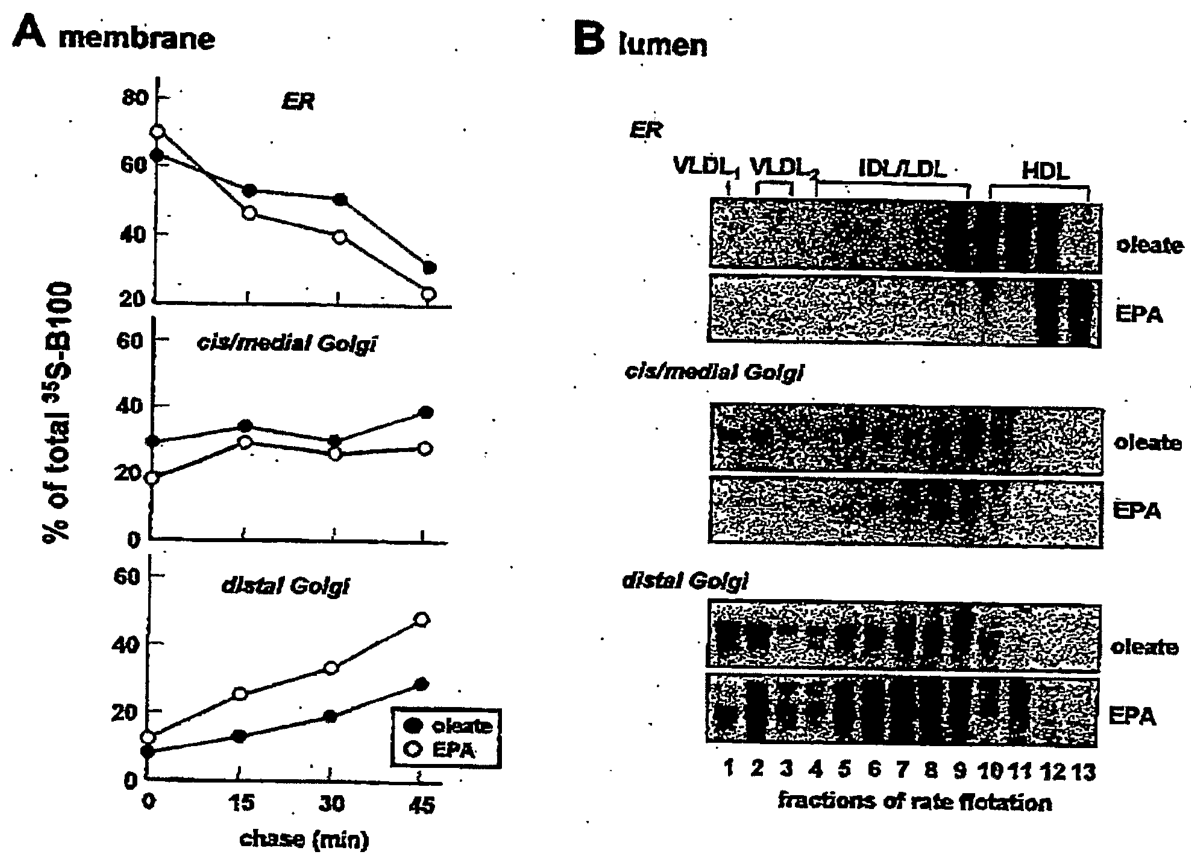
A membrane
ER
cis/medial Golgi
distal Golgi
% of total 35S-B100
80
60
40
20
0
15
30
45
chase (min)
oleate
EPA
B lumen
ER
VLDL1 VLDL2 IDL/LDL HDL
oleate
EPA
cis/medial Golgi
oleate
EPA
distal Golgi
oleate
EPA
1 2 3 4 5 6 7 8 9 10 11 12 13
fractions of rate flotation

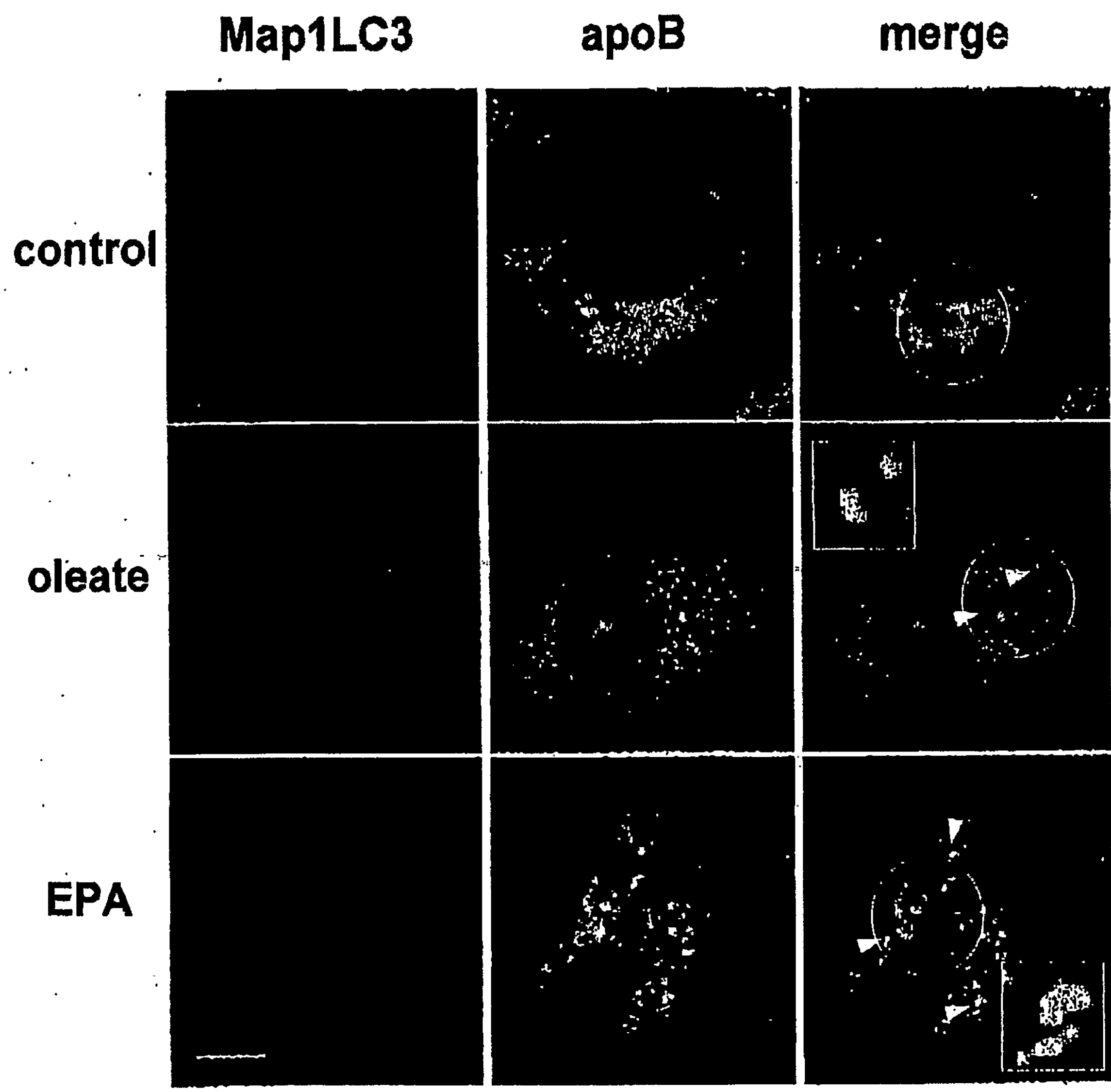
Map1LC3
apoB
merge
control
oleate
EPA

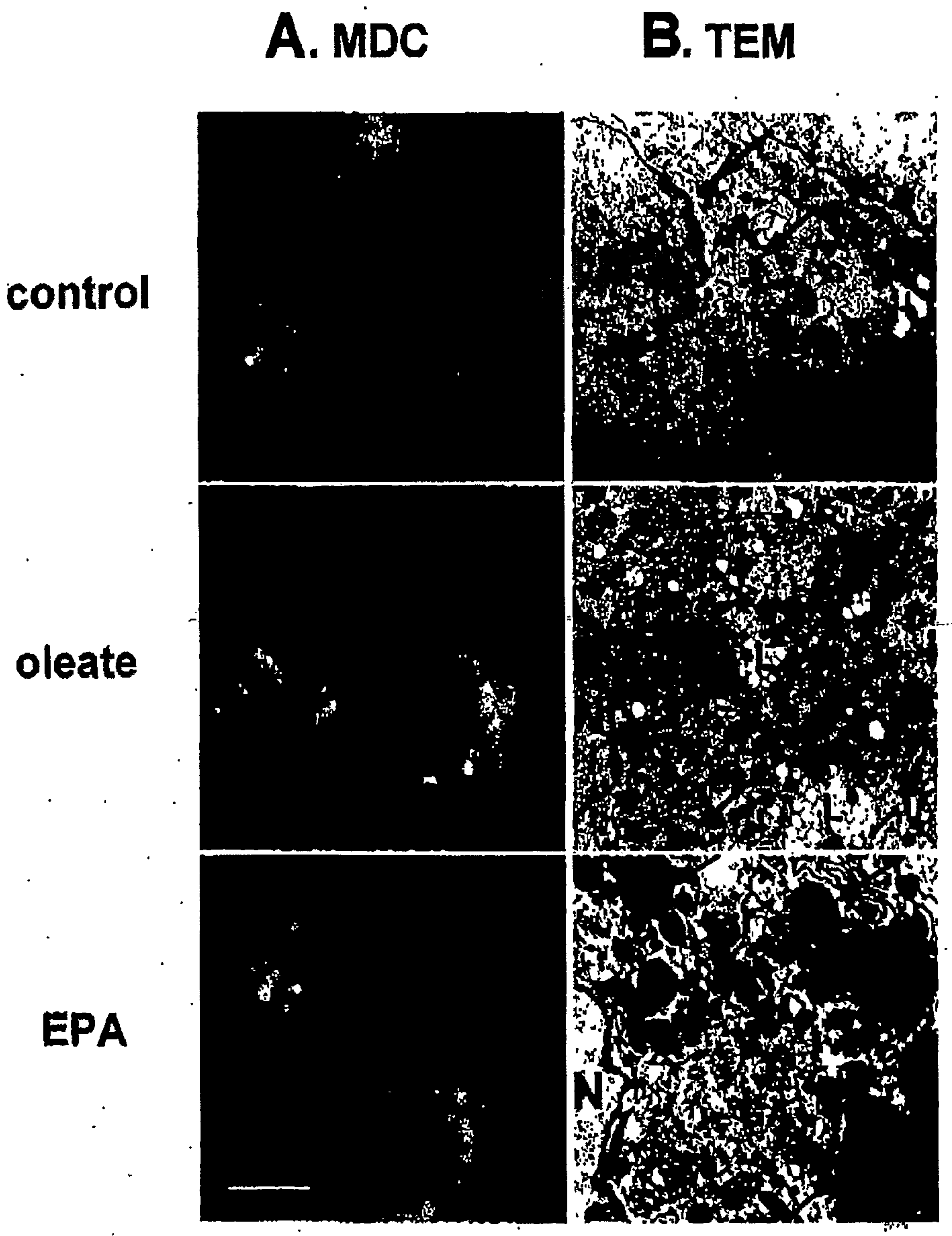
A. MDC
B. TEM
control
oleate
EPA
N

Tran et al., Fig. 5

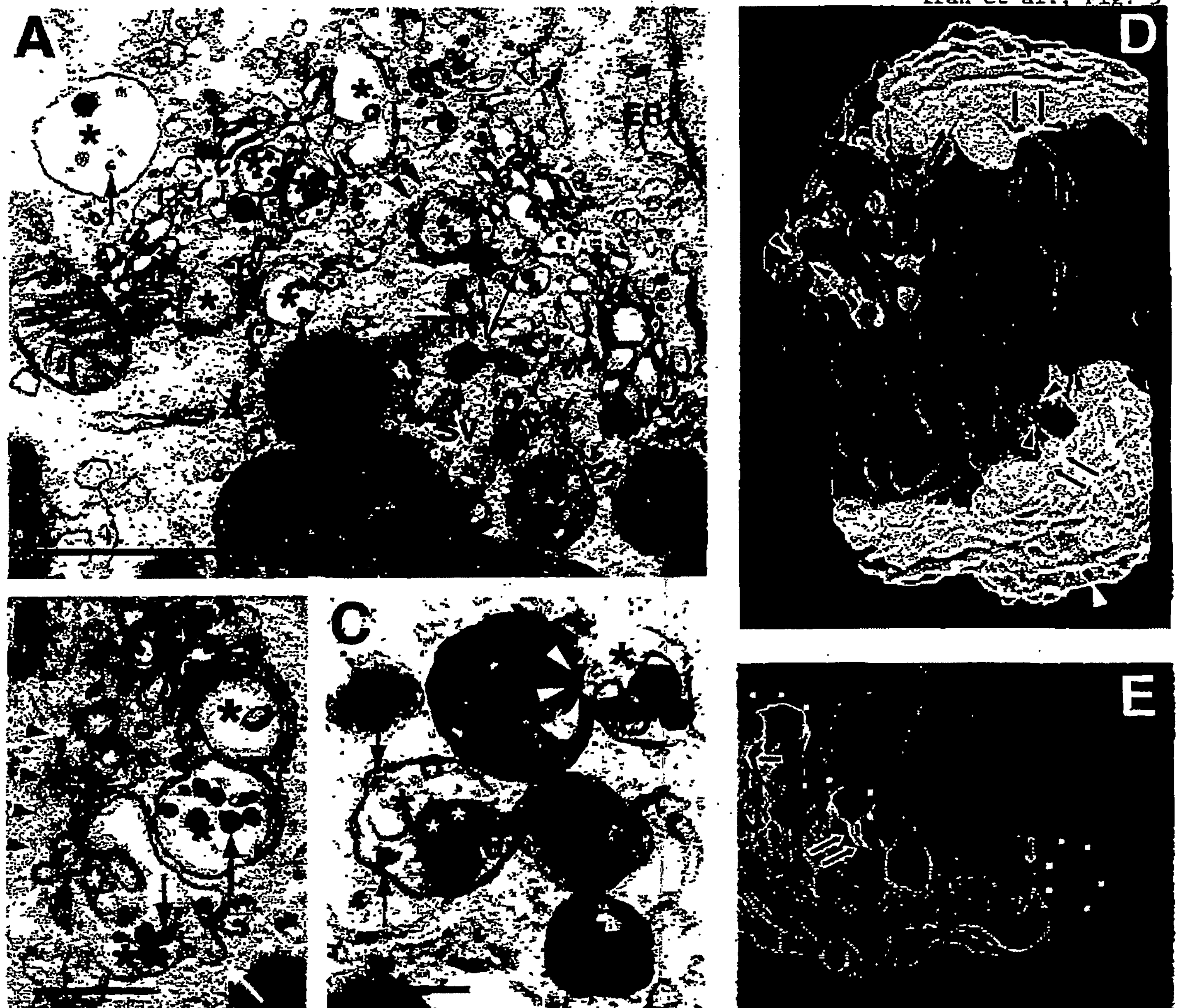

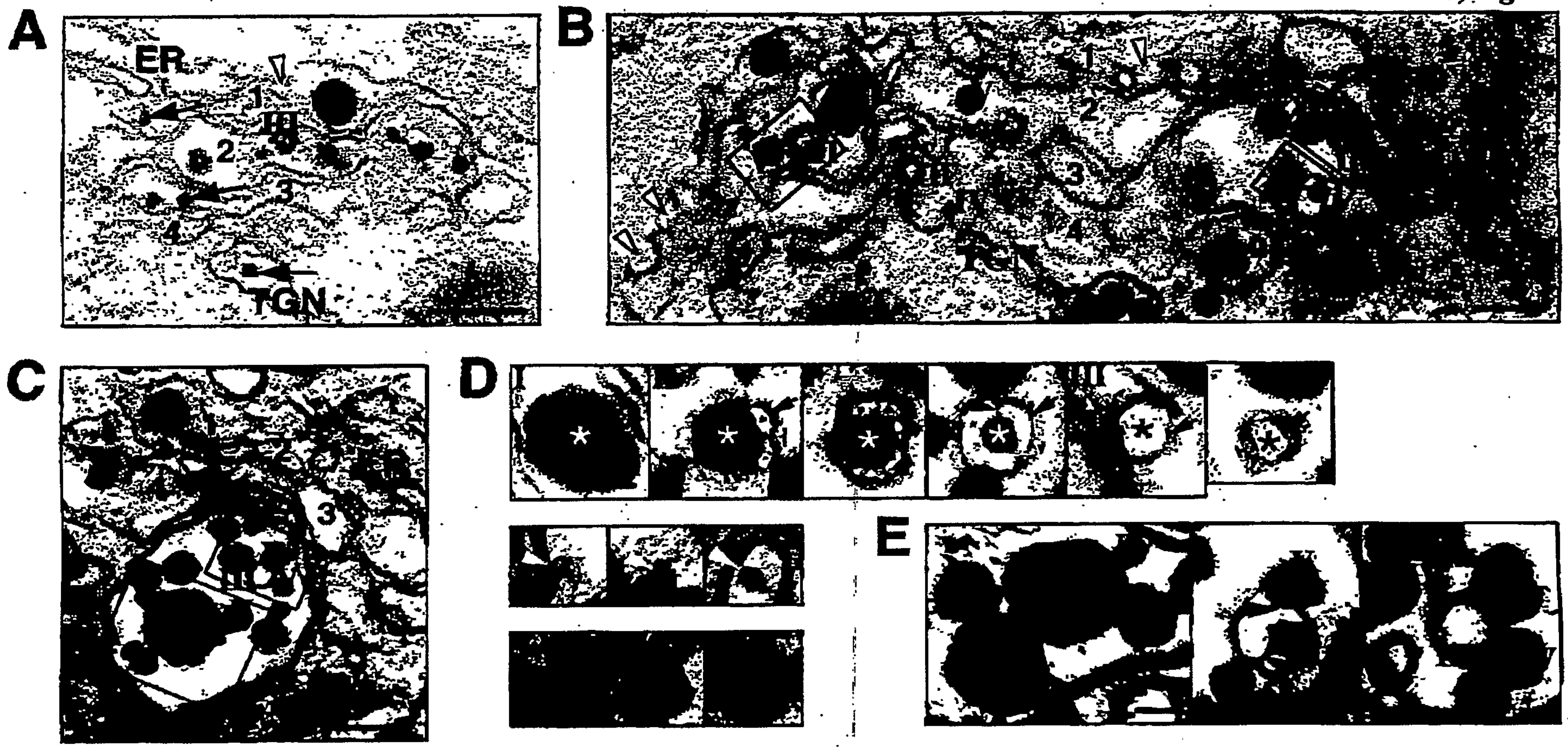
A
ER
1
2
3
4
TGN
B
1
2
3
4
C
3
D
E

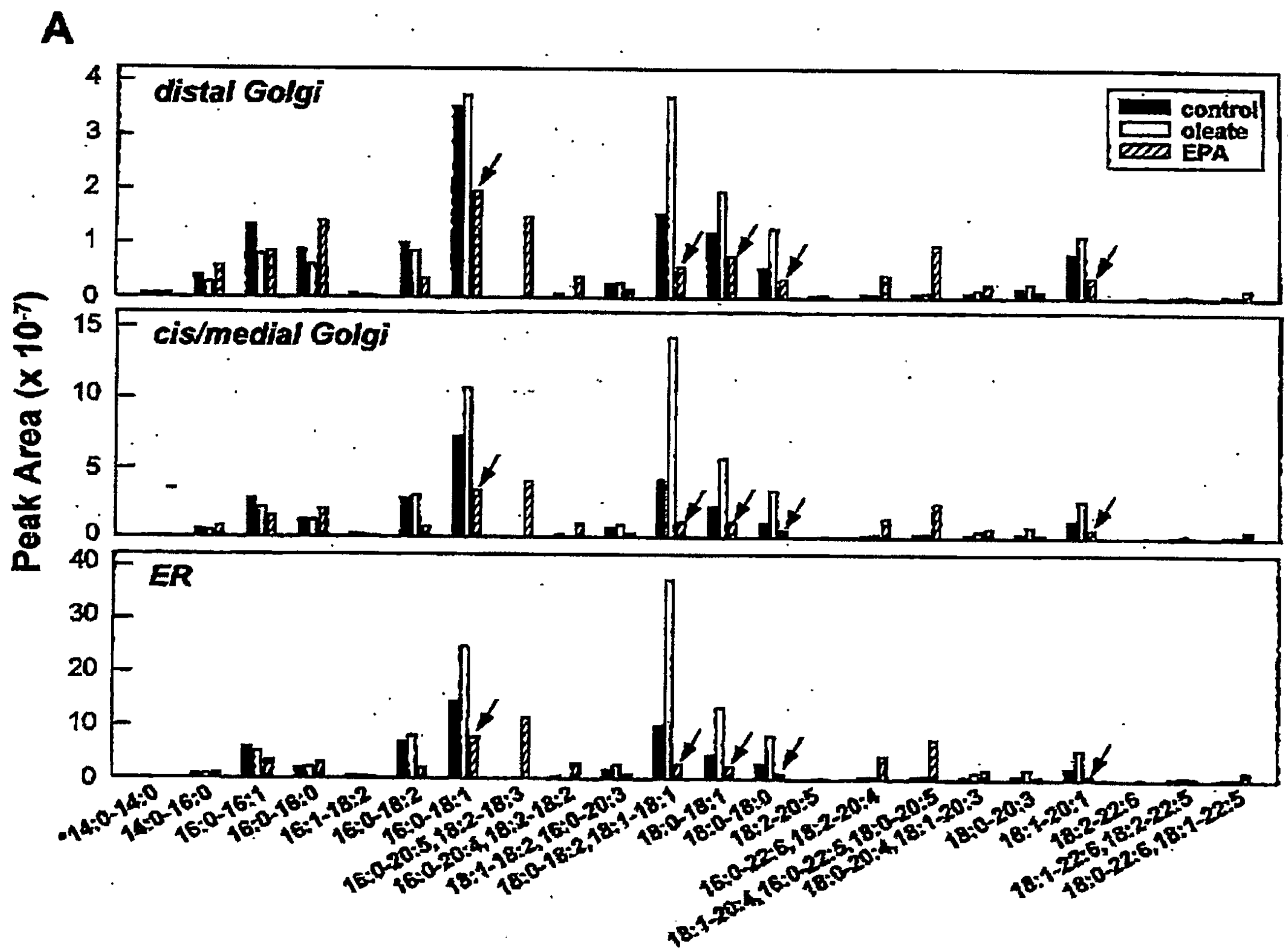
A
distal Golgi
cis/medial Golgi
ER
control
oleate
EPA
Peak Area (x 10-7)
4
3
2
1
0
15
10
5
0
40
30
20
10
0
14:0-14:0
14:0-16:0
16:0-16:1
16:0-16:0
16:1-18:2
16:0-18:2
16:0-18:1
16:0-20:5,18:2-18:3
16:0-20:4,18:2-18:2
18:1-18:2,16:0-20:3
18:0-18:2,18:1-18:1
18:0-18:1
18:0-18:0
18:2-20:5
16:0-22:6,18:2-20:4
18:1-20:4,16:0-22:5,18:0-20:5
18:0-20:4,18:1-20:3
18:0-20:3
18:1-20:1
18:2-22:6
18:1-22:6,18:2-22:5
18:0-22:6,18:1-22:5

B

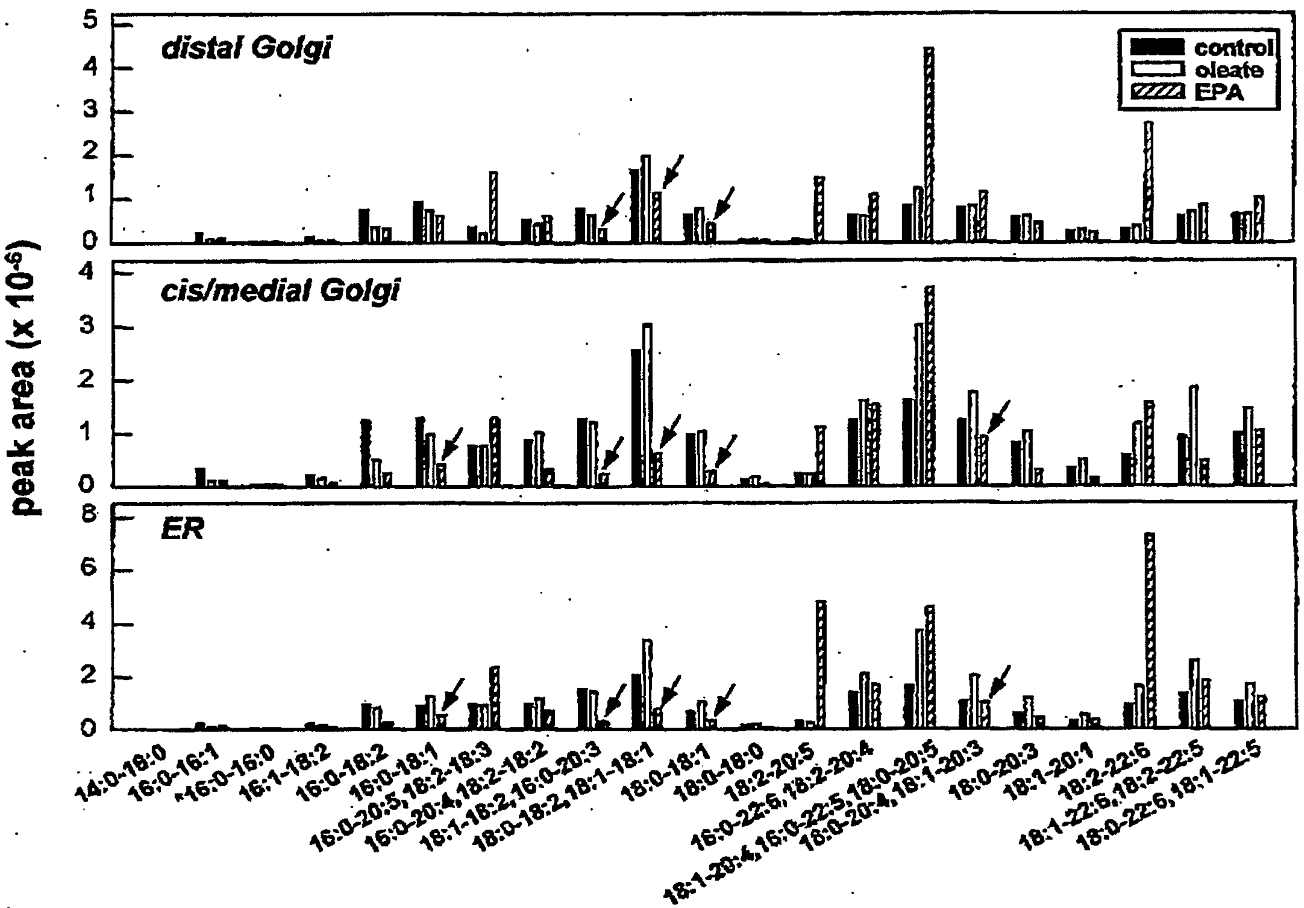
distal Golgi
cis/medial Golgi
ER
peak area (x 10-6)
control
oleate
EPA
14:0-18:0
16:0-16:1
16:0-16:0
16:1-18:2
16:0-18:2
16:0-18:1
16:0-20:5,18:2-18:3
16:0-20:4,18:2-18:2
18:1-18:2,16:0-20:3
18:0-18:2,18:1-18:1
18:0-18:1
18:0-18:0
18:2-20:5
16:0-22:6,18:2-20:4
18:1-20:4,16:0-22:5,18:0-20:5
18:0-20:4,18:1-20:3
18:0-20:3
18:1-20:1
18:2-22:6
18:1-22:6,18:2-22:5
18:0-22:6,18:1-22:5

Tran *et al.* Fig. 8

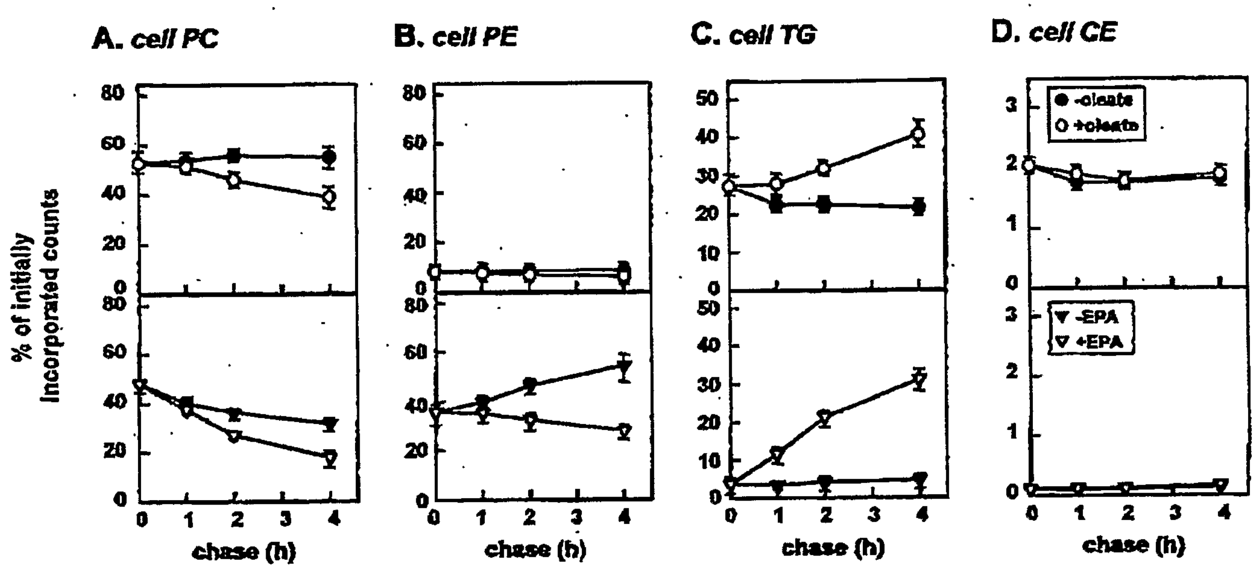

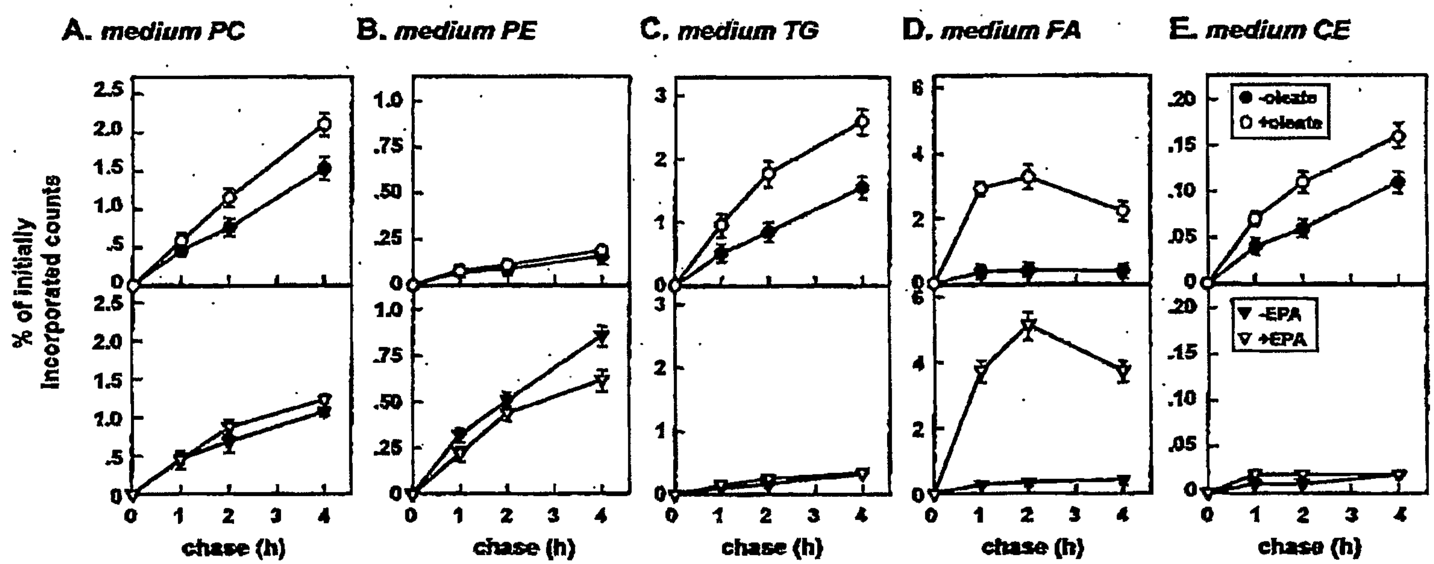
A. medium PC
B. medium PE
C. medium TG
D. medium FA
E. medium CE
% of initially
incorporated counts
chase (h)
● -oleate
○ +oleate
▼ -EPA
▽ +EPA

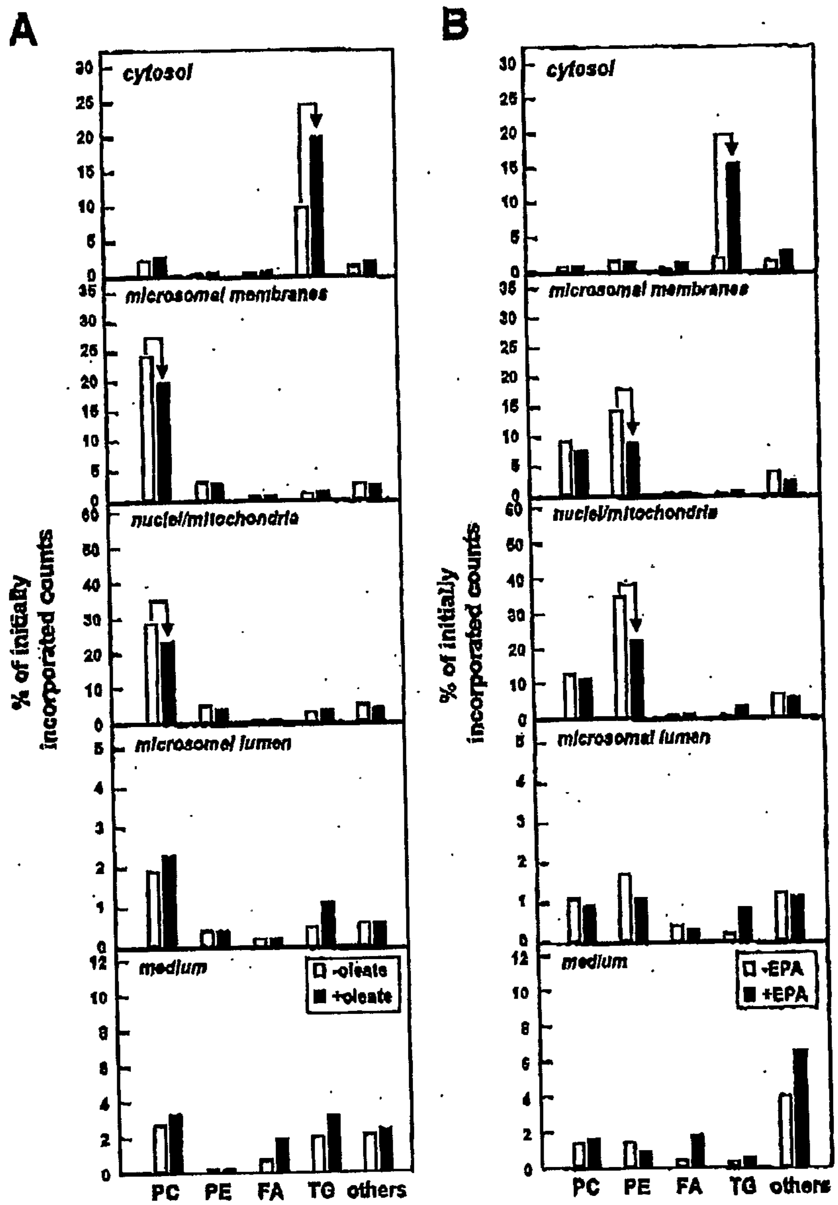
A
B
cytosol
microsomal membranes
nuclei/mitochondria
microsomal lumen
medium
% of initially incorporated counts
-oleate
+oleate
-EPA
+EPA
PC
PE
FA
TG
others

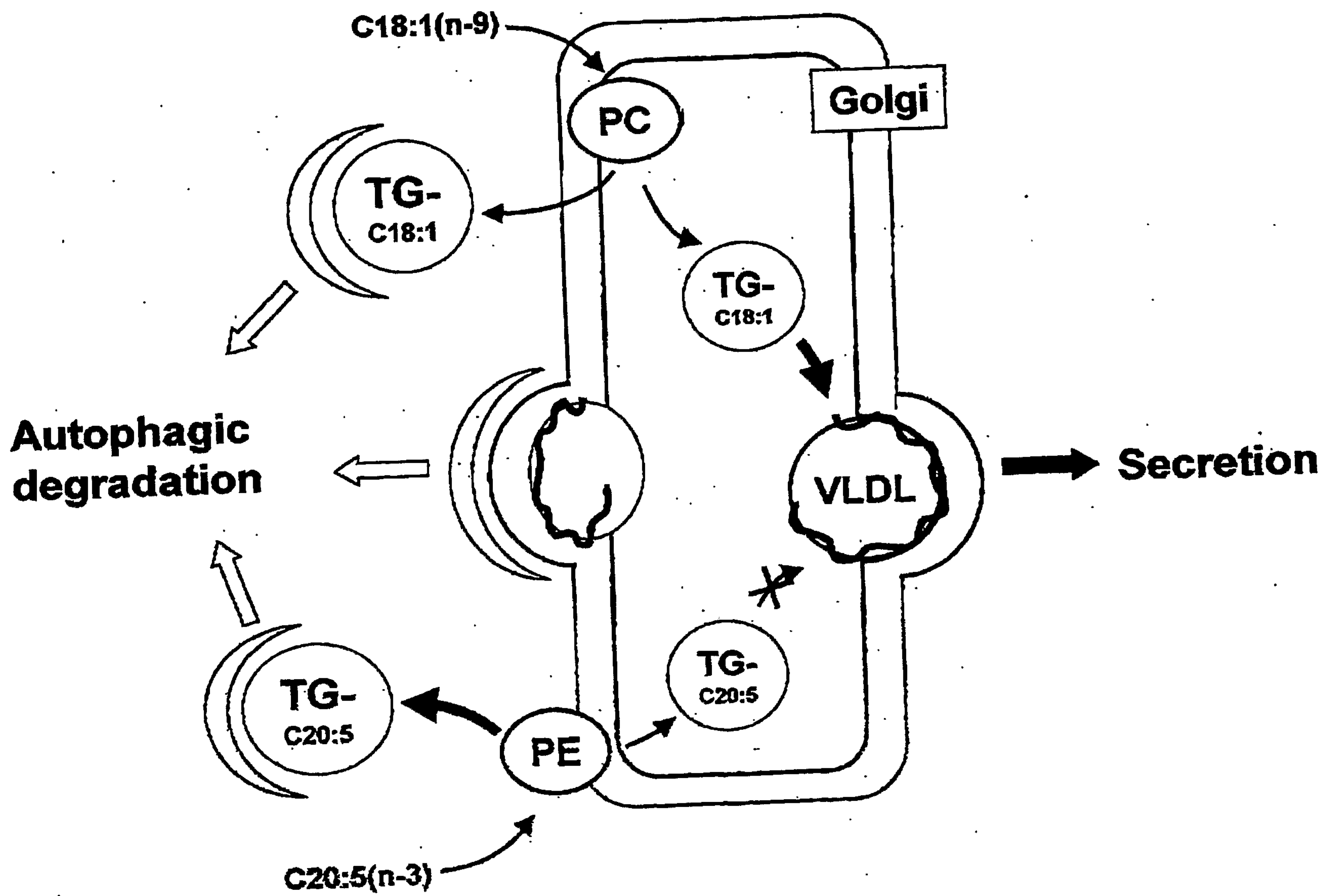
C18:1(n-9)
PC
Golgi
TG-
C18:1
TG-
C18:1
Autophagic degradation
VLDL
Secretion
TG-
C20:5
TG-
C20:5
PE
C20:5(n-3)